What *Drives* the Efficiency in Ridesharing Markets? Evidence from Austin, Texas

Motaz Al-Chanati*   Vinayak Iyer†

May 2022

Abstract

In decentralized transportation markets, search and match frictions lead to inefficient outcomes. Ridesharing platforms, which act as intermediaries in these markets, improve upon the status quo along two dimensions: surge pricing and centralized matching. Through the lens of a structural model, we show that both surge and matching are critical in making the market more efficient, albeit for different reasons. Surge plays a crucial role in inducing supply, primarily during late nights, while centralized matching mitigates search and match frictions throughout the day. Finally, we show that a more flexible pricing rule can generate even larger welfare gains.

Keywords: *ridesharing, surge pricing, centralized matching, dynamic games, search frictions*

JEL Classification: *L91, R41, D43, C73*

*Cornerstone Research. Email: motaz.al-chanati@cornerstone.com.

†Columbia University, Department of Economics. Email: vi2137@columbia.edu.

Acknowledgements: We are extremely grateful to Bernard Salanié, Don Davis, Suresh Naidu, Pierre-André Chiappori, Cailin Slattery, Tobias Salz and Michael Best for their valuable advice and support. We thank Yining Zhu for her initial contributions on this project. We are also grateful to Guy Aridor, Iain Bamford, Maggie Shi, Dilip Ravindran, Shoumitro Chatterjee, Anjali Priya Verma and participants at Columbia's Applied Micro Theory Colloquium, IO Colloquium, Trade Colloquium, Delhi School of Economics and UEA 2020 for their feedback. We would also like to acknowledge that most of the work reported on in this paper was performed at the Habanero HPC at Columbia University. Motaz Al-Chanati coauthored this paper before joining Cornerstone Research. The views expressed herein are solely those of the authors who are responsible for the content, and do not necessarily represent the views of Conerstone Research. All errors are our own.

1 Introduction

Many decentralized markets are inefficient due to the presence of search and match frictions. Transport, labor, and housing markets are well-known examples of this. As a result, intermediaries exist in many of these markets to reduce these frictions. Intermediaries arguably improve efficiency through two mechanisms: facilitating easier matching of buyers and sellers and by organizing the pricing structure in the market.[1] However there is relatively little quantitative evidence on the efficiency gains induced by these matching and price mechanisms and how market participants respond to them.

This paper studies the case of RideAustin – a ridesharing company in Austin, Texas – to understand the role and relative contribution of matching and pricing in solving different market inefficiencies and improving market outcomes. In transportation markets, these inefficiencies broadly take two forms: static and dynamic inefficiencies. Static inefficiencies arise when, due to search frictions, riders are unable to match with drivers at a particular point in time. We measure this as the proportion of rides requested which remained unfulfilled. Dynamic inefficiencies arise when riders choose to travel to relatively low demand areas, resulting in a suboptimal spatial distribution of supply. Similarly, the search, entry, and exit decisions of drivers may also distort the spatial distribution of supply and induce further dynamic inefficiencies. We measure this dynamic inefficiency by the time drivers spend searching for passengers.

In the particular context of ridesharing, the two instruments used by intermediaries such as Uber, Lyft, and RideAustin are surge pricing and centralized matching. Each of these two features is important in overcoming the inefficiencies in the market albeit for different reasons. Surge (or dynamic) pricing allows fares to vary with market conditions, unlike the typical fixed rates of taxis.[2] As a result, it may play a crucial role in mitigating both static and dynamic inefficiencies by aiming to create a balanced pattern of demand and supply. Higher prices incentivize drivers to enter the market as well as to target their search towards specific locations. These higher prices also allocate rides to consumers with the highest valuation. In two-sided markets such as ridesharing, prices are crucial in ensuring participation by both sides of the market.[3] Centralized matching connects riders and drivers through a common platform (the app) without these two agents having to physically interact. Centralized matching potentially mitigates static inefficiencies

[1] Intermediaries like eBay, Airbnb and Uber are examples of intermediaries who organize the matching and price structure in existing markets. All these companies provide a platform for buyers and sellers to match with each other. Prices on eBay are determined through auctions; sellers set their own prices on Airbnb; Uber sets prices centrally. Einav et al. (2016) give an overview of these peer-to-peer markets.

[2] Surge pricing refers to a surge factor or multiplier (greater than 1) that is multiplied to a base fare.

[3] This channel has often been highlighted as the key factor in the efficiency gains of ridesharing markets. Its proponents emphasize that flexible pricing allows for improved allocations, resulting in higher consumer welfare (Hall et al., 2015). Opponents of surge pricing, however, argue that it acts as a form of price discrimination against riders (Dholakia, 2015), while being ineffective at incentivizing drivers (Diakopoulos, 2015; Lee et al., 2015).

by reducing the search frictions faced by riders and drivers. This likely induces efficiency gains over taxi markets, where a match occurs only if a rider can successfully hail a vacant driver who is in the same location at the same time.

To quantify how much surge and matching overcome these market inefficiencies and to understand the specific role played by each feature, we estimate a structural model of the ridesharing market. We use data from RideAustin, which had the largest market share in Austin during our sample period of October 2016 to May 2017.[4][5] Using this data we first establish key empirical facts about the role of surge and matching. We show that surge pricing influences drivers to target high demand areas by "chasing" the surge. Moreover, surge is concentrated in downtown Austin on weekends and occurs in less than 15% of all observed trips. We also establish that the search frictions faced by drivers in RideAustin are significantly lower compared to the New York City taxi market.

Our model includes four components: (1) dynamically optimizing drivers choosing whether to enter, which location to search in, and whether to exit; (2) stochastic demand that is responsive to price and waiting time; (3) a matching technology that assigns riders to drivers across the city; and (4) a pricing algorithm which sets the surge factor for a location at a point in time. This builds upon Buchholz (2020) and Fréchette et al. (2019) who, respectively, model the intensive and extensive margin of labor supply of taxi drivers in New York City. We do not directly observe the pricing and matching algorithms used by RideAustin and therefore, before estimating the key parameters of our model, we approximate the pricing and matching algorithms used by the company. Our approximations match the patterns we observe in the data well. We then estimate the demand for rides using an instrumental variable (IV) approach which gives us estimates for the price and waiting time elasticity of demand. We finally estimate the key parameters governing the supply side of our model using simulated method of moments. Our estimated model is able to match both targeted and non-targeted moments well.

To empirically quantify the welfare contribution of surge and matching – as well as uncover the channels through which they solve market inefficiencies – we conduct policy counterfactuals and find three main results.

First, we show that both surge pricing and centralized matching are crucial in increasing consumer surplus, driver profits, and reducing the proportion of unmet demand (our measure of static inefficiency). In particular, we find that while centralized matching reduces unmet demand and induces welfare gains irrespective of the time of the day, surge pricing is most crucial late at night. Under a system without surge pricing, consumer surplus slightly increases by 4% during the af-

[4] In May 2016, the Austin city council passed a council ordinance requiring fingerprint-based background checks for ridesharing drivers. In response, Uber and Lyft ceased operations in the city. RideAustin entered the market and was one of the two major companies in the market till Uber and Lyft returned in May 2017.

[5] Tarduno (2021) uses the same data to study the congestion effects of ridesharing companies.

ternoon, while it falls dramatically by 65% at night. Surge pricing incentivizes drivers to enter the market, especially at night when drivers highly value their outside option. This in turn makes it more likely for riders to be successfully matched to a driver. Thus, while centralized matching reduces static inefficiencies by eliminating match frictions, surge pricing mitigates static inefficiencies through its effects on driver entry. We also find large spatial heterogeneity in consumer surplus in the absence of surge or centralized matching, with the suburbs disproportionately worse off relative to downtown Austin. These results lead us to two policy recommendations. Seemingly pro-rider policies, such as banning or capping surge pricing, may in fact harm consumers. In contrast, taxis who wish to compete with ridesharing companies should primarily focus on introducing a matching technology rather than introducing surge pricing.[6]

Second, we assess whether the platform could further increase welfare by changing its pricing or matching rules and how these could mitigate dynamic inefficiencies. We find that higher surge prices reduce consumer surplus but increase driver profits. Moreover, there is somewhat limited scope for improving the matching technology. Match frictions can only be reduced so much, whereas there are many different pricing schemes the platform could use. We study one option that we refer to as "flexible surge", which allows for the surge factor to go below one. Ridesharing companies typically use one-sided surge: it only becomes activated in areas of relatively *high* demand.[7] Fully flexible prices should also give discounts to places with relatively *low* demand. We find that this simple pricing strategy significantly increases welfare for all agents. These price discounts induce more riders into the market, which in turn allows incumbent drivers to be better matched to riders. As a result, flexible prices creates a more balanced pattern of demand and supply across locations, thereby reducing the vacant time between rides (our measure of dynamic inefficiency).

Finally, we evaluate how our results would change under the driver compensation schemes used by companies such as Uber and Lyft. RideAustin used a fixed-fee compensation scheme in which the company took $0.99 for each completed ride, with the remaining fare going to the driver. Under a counterfactual world with Uber's driver compensation scheme, we find similar qualitative patterns but lower total welfare as compared to the benchmark model of using RideAustin's compensation scheme. The results indicate that if a ridesharing platform does not internalize the effects of its policies, it may create a distortion that prevents the market from achieving the socially optimal outcome.

[6] Cities like New Delhi and Honolulu aimed to regulate the surge pricing feature of ridesharing apps. On the other hand cities like New York are planning to introduce surge pricing for traditional taxis to increase competition with Uber and Lyft.

[7] The surge factor in Uber as well never falls below one making it only flexible upwards, for example, as shown in Castillo (2019).

1.1 Related Literature

Our paper contributes to the empirical literature on transportation, dynamic pricing, and intermediaries in markets with search and match frictions.

First, our paper contributes to the growing literature on ridesharing/taxi markets. We quantify and decompose the efficiency gains arising from different features of ridesharing companies. We also uncover the margins that each of these features affects and the inefficiencies that they solve. Methodologically, our model builds on Buchholz (2020) and Fréchette et al. (2019) who study the New York City taxi market and conduct counterfactuals to assess whether, respectively, different pricing schemes and a platform like Uber can increase welfare. In particular, Buchholz (2020) develops a structural model with drivers searching the city, but without entry and exit decisions. In contrast, Fréchette et al. (2019) models drivers' entry and exit decisions, but without strategic search. We extend the Buchholz (2020) model to incorporate both surge pricing and centralized matching, and allowing drivers to strategically choose to enter, exit, and search. Our paper reinforces and extends the findings of Buchholz (2020) and Fréchette et al. (2019) by not only explicitly modeling the features of a ridesharing market but also documenting the role and joint importance of centralized matching and surge pricing in increasing welfare and solving the static and dynamic inefficiencies arising in ridesharing markets.

Brancaccio et al. (2020) study the decentralized dry bulk shipping industry and also document large gains from frictionless matching and optimal taxes. The notion of thick/thin and pooling externalities developed in their paper are similar to the static and dynamic inefficiencies we focus on. A key difference is that we allow entry and exit of drivers (carriers in their setting) which is an important aspect of the ridesharing market (and the gig economy, more generally). Our paper complements their findings by highlighting the importance of centralized matching and surge pricing in mitigating static inefficiencies and increasing welfare. In particular, surge pricing mitigates static inefficiencies by incentivizing driver entry. Furthermore, we also show that fully flexible pricing reduces dynamic inefficiencies in transport markets by creating a balanced pattern of demand and supply across locations.

Another related paper is Castillo (2019), who studies Uber in Houston, Texas and focuses on distributional consequences of surge pricing. As in our analysis, he also finds that consumer welfare falls when surge pricing is removed. We both find that higher surge factors result in higher average prices and increase driver profits. Substantively, our papers differ along two key dimensions. First, his paper focuses on surge pricing and its distributional consequences for high and low income riders, while we focus on the relative contribution and role of centralized matching and surge pricing in solving market inefficiencies. Our results indicate that matching plays an equal (if not more important) role in driving the efficiency gains of ridesharing platforms. Second, we model drivers as fully rational and forward-thinking, whereas he models driver decisions using a heuristic approach. In particular, we explicitly account for how surge pricing and matching affects the drivers' value function. Castillo (2019), however, is able to observe when agents log into the app (something that we cannot observe in our setting), which allows him to estimate short-run and long-run elasticities in response to changes in prices.

Other papers studying various features of ridesharing platforms such as Ghili and Kumar (2020) and Shapiro (2018) focus on the role of density in the success of ridesharing platforms. Rosaia (2020) studies how mergers between competing platforms affects traffic congestion in the city. Liu et al. (2019) study the role of centralized matching in increasing efficiency in a decentralized ridesharing market. Another set of papers estimate the flexibility of labor supply among ridesharing drivers (Chen et al., 2019; Angrist et al., 2017). Our paper complements these studies by finding large within-day variation in the flexibility of labor supply for drivers, thus highlighting the importance of surge pricing in inducing drivers to enter the market. Finally, our paper complements other studies of ridesharing platforms such as (Cohen et al., 2016), who estimate consumer surplus, (Berger et al., 2018; Hall et al., 2018) who study how ridesharing changes traditional transport markets, and Buchholz et al. (2020) who estimate consumer valuations of time. Our focus is on developing a structural model of a ridesharing platform, as well as understanding how this intermediary has made an existing market (the taxi market) more efficient.

Second, our paper contributes to the literature on dynamic pricing in a variety of markets (Joskow and Wolfram (2012); Wolak (2011); Lazarev (2013); Williams (2020)). In addition, there is a recent theoretical literature studying optimal pricing in ridesharing platforms (Bimpikis et al. (2019), Besbes et al. (2020), Castillo et al. (2017)). Our paper empirically verifies key theoretical properties of optimal pricing in ridesharing networks developed by Bimpikis et al. (2019) and Besbes et al. (2020). The key idea in these papers is that the demand and supply patterns induced by the optimal pricing rule should be "balanced" across locations. The surge factors used by ridesharing companies such as Uber, Lyft, and RideAustin are bounded below by one, i.e. they are only flexible upwards. By modifying the existing pricing rule to allow the surge factor to go below one for areas with relatively low demand, we simulate large welfare gains for all consumers and drivers. These results show that fully flexible surge pricing is able to solve the dynamic inefficiencies of transport markets by balancing demand and supply across locations. This ensures drivers spend less time searching for passengers between trips.

Finally, our paper also contributes to the literature on the role and importance of intermediaries in markets with search and match frictions. Gavazza (2016), Hendel et al. (2009), and Salz (2020) study the role of intermediaries in improving market outcomes in the airline, housing, and waste markets, respectively. Our paper also is related to the literature on two-sided platforms (Rochet and Tirole (2003), Rochet and Tirole (2006)). Einav et al. (2016) provides a detailed overview of peer-to-peer markets. Farronato and Fradkin (2018) similarly analyzes the welfare impact of a new technological platform (Airbnb) on the housing market.

The rest of the paper is organized as follows. Section 2 provides an overview of our setting and data, as well as motivating summary statistics. Section 4 details our model of the ridesharing market. We then outline how we estimate this model in Section 5. Finally, we present our results and counterfactuals in Sections 6 and 7.

2 Setting and Data

We study the case of RideAustin, a ridesharing company based in Austin, Texas, for the period of October 2016 to May 2017.

2.1 Background

In May 2016, the Austin city council passed a council ordinance requiring fingerprint-based background checks for ridesharing drivers. In response, Uber and Lyft ceased operations in the city. This led to many new companies entering to fill the gap, with RideAustin being the largest player in the market. Tarduno (2021)[8] A statewide law eliminating the background check requirement passed on May 29, 2017. This superseded Austin's local rules, after which Uber and Lyft shortly returned to the city.

In terms of app interface and functionality, RideAustin was quite similar to Uber. Like Uber at the time, RideAustin had surge pricing at discrete rates (in increments of 25 cents) and surge was mandatory.[9] Unlike Uber, RideAustin did not offer pooled (multi-passenger) rides like UberPool or Lyft Shared. Another major difference is that RideAustin was a registered 501(c)(3) non-profit which only charged drivers a flat \$0.99 fee per ride. The rest of the trip fare went to the drivers.[10] Uber, on the other hand, charges its a drivers a percentage commission, typically at a rate of 25% of the total fare. This is a major advantage in our setting because it allows us to focus on rider and driver welfare and abstract away from the platform's profit maximization problem.

[8]RideAustin had approximately 50% market share in Austin's ridesharing market during the period in which Uber and Lyft were not present. The second largest competitor at the time was Fasten, which ceased operations in the U.S. in March 2018.

[9]In contrast, RideAustin's competitor Fasten had optional surge which allowed a rider to move to the front of the waiting queue by accepting the surged price.

[10]The revenue per trip for the driver is $\pi = f(\delta, \tau) \times s - 0.99$, where $f(\delta, \tau)$ is the unsurged fare (a function of the trip's distance δ and time taken τ) and s is the surge factor. $s = 1$ represents an unsurged ride.

2.2 Data

We estimate our model using data from RideAustin. The company published their ride-level data for June 2016 to April 2017 – a time when both Uber and Lyft were not operational in Austin. The publicly available data includes 1.2 million rides with over 4,000 distinct drivers. For each ride, we observe a unique driver identifier, the total fare, trip distance and surge factor for that trip, as well as the coordinates and times of the pick-up and drop-off. We supplement this with additional data obtained from RideAustin, which also included data on rides over a longer time period (July 2016 to October 2019). The additional data provides the time and driver's location when they were dispatched to pick up a passenger, allowing us to track how far a driver had to travel to meet the rider. We also obtained the geographic definitions used by the company to set surge factors, as well as the value of surge in each area every 5 minutes for December 2016 to May 2017. A key limitation of our data is that we only observe *matched* rides. This means we do not observe requested trips that go unmatched or that are cancelled by either party. A larger concern is that we cannot observe drivers while they are not engaged in a trip, i.e. we cannot directly observe how they search while they do not have a passenger. However, as we discuss in section 3.3, the dispatch coordinates will help us in overcoming this data limitation.

For our analysis, we focus on rides occurring between October 2016 and May 2017. This eliminates RideAustin's start-up period of growth as well as its decline following the return of Uber and Lyft. As Figure (A1) shows, this best captures when RideAustin is in equilibrium as a major market player. Figure (A2) shows further restrictions we make to ensure that our data represents a typical week of ridesharing.

3 Summary Statistics

In this section, we present key empirical patterns of demand, supply, prices, and matching in this ridesharing market. We use these patterns in the data to motivate the features of the model. We also discuss how these patterns will help us identify the parameters in our model.

To analyze the data, it is useful to standardize the time and physical space that our data covers. We define a "day" as representing a 24 hour period starting at 4:00 a.m. We begin the day at 4 a.m. rather than midnight for two reasons. First, rides in the early morning are best thought of as late night activity continuing from the previous day's evening rather than events separate from it. Second, 4:00 a.m. is when the least number of rides within a day occur, which provides a reasonable point to divide the day. Furthermore, we divide the city of Austin into equally-sized hexagons that are approximately 0.9 kilometers wide using Uber's H3 geospatial indexing system. We choose to divide the city in such a way since a main feature of our model is to characterize notions of *local* demand and supply.

3.1 Spatial and Temporal Distribution of Demand and Surge

We first determine where and when trips and surged rides most often occur in our data. We find that the demand for rides, as well as the probability of rides being surged, is concentrated in downtown Austin and on weekends. We also find that most rides are unsurged, with surge accounting for a quarter of rides in high activity areas and times.

In Figure (1), we plot the spatial distribution of trip start locations. The outline superimposed on the map indicates the neighborhoods we use to aggregate the hexagons. This approximately matches the administrative boundaries of the city of Austin.[11] Rides occurring outside these neighborhoods are infrequent; 94% of rides start *and* end within our defined neighborhoods, so we restrict all further analysis to only those rides. Even within the city, there is still large spatial variation in the frequency of rides. We see that the overwhelmingly majority of trips begin in downtown Austin, the small central neighborhood depicted on the map. This is an area where many amenities, such as bars and restaurants, are located. Rides in the outer suburban neighborhoods are far more infrequent.

Next, we plot the spatial distribution of the probability of surge occurring. For each hexagon, we calculate the ratio of the total number of surged rides (rides that had a surge factor greater than 1) starting in that hexagon relative to the total number of rides starting from that hexagon. We also calculate this ratio for rides ending in each hexagon and then plot the spatial distributions of these ratios in Figure (2). We find that while most of the rides are unsurged, there is a correlation between surge and trip volume. The probability of surge generally peaks for rides that start around the central downtown area, whereas rides beginning in the outer suburban areas are rarely surged. In contrast, there is no distinct pattern for where surged trips ends. This suggests that surge is only a function of conditions in your pick-up location, and not your destination.

Figure (2) also shows that surge is not a frequent occurrence. In the downtown neighborhood, where most rides (and most surged rides) occur, surge occurs in only 23% of rides. The relative infrequency of surge pricing is highlighted in Table (1) which plots the frequency distribution of surge factors. We find that 86% of rides in our data have a surge factor of 1, i.e. they are unsurged. The remaining rides have a surge factor associated with them, with most of these occurring in the two lowest surge factors of 1.25 and 1.50. On Fridays and Saturdays (the highest activity days of the week), unsurged rides fall to 78% in our data. These statistics are similar to Castillo (2019), who finds that 77% of Uber rides in Houston are unsurged.[12] Therefore, while surge pricing is an

[11] See Appendix B for an overview of the geographic units used in the analysis.

[12] In that context, Uber had a monopoly of the Houston ridesharing market. An earlier version of this paper used Uber data from San Francisco and he finds that 86% of Uber rides in San Francisco were unsurged.

Figure 1: Distribution of Trips (by Start Location)

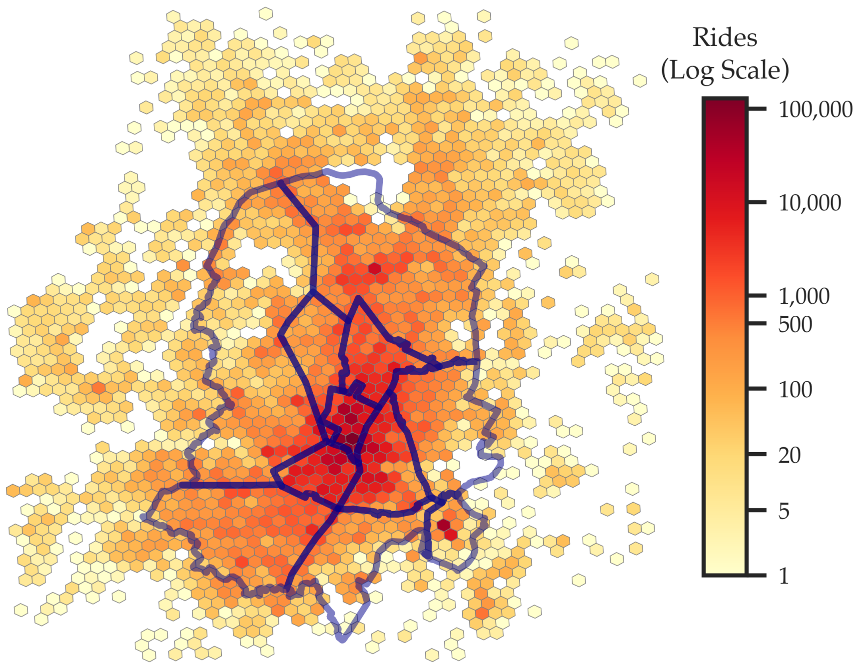

often-discussed aspect of ridesharing, in reality, the majority of rides go unsurged.

We next look at the temporal distribution of rides and surge. Panels (a) and (b) in Figure (3) show the distribution of rides and the probability of surged rides across a typical week. We find that rides are most likely to occur on Friday and Saturday nights with a sharp drop-off after 2 a.m., which is when bars in Austin are mandated to close. Even though the closing time is a completely anticipated event, we find that rides are most likely to be surged at 2 a.m. on Friday nights and Saturday nights with nearly 60-70% of observed rides being surged in this time period.[13] Rides are also likely to be surged around the evening, which corresponds to the evening post-work traffic rush on weekdays. These stylized facts imply that accounting for intra-day variations in demand and supply is important when modeling and estimating the ridesharing market.

3.2 Match Frictions in Ridesharing

Search frictions in a ridesharing market are relatively low. As a benchmark, we show that frictions in our setting are significantly lower compared to the New York City taxi market. Figure (4) shows that drivers' vacancy rate (time they spend searching for a ride as a percentage of total

[13]A 2016 column in Forbes observed that: "Bars in Austin are also required, per Texas state law, to close at 2am. There are some dance clubs that stay open after that, but they can't serve alcohol. This means that after last call on 6th Street, thousands of people flood from the bars at once, crowding sidewalks and causing traffic jams."

Figure 2: Distribution of Surge

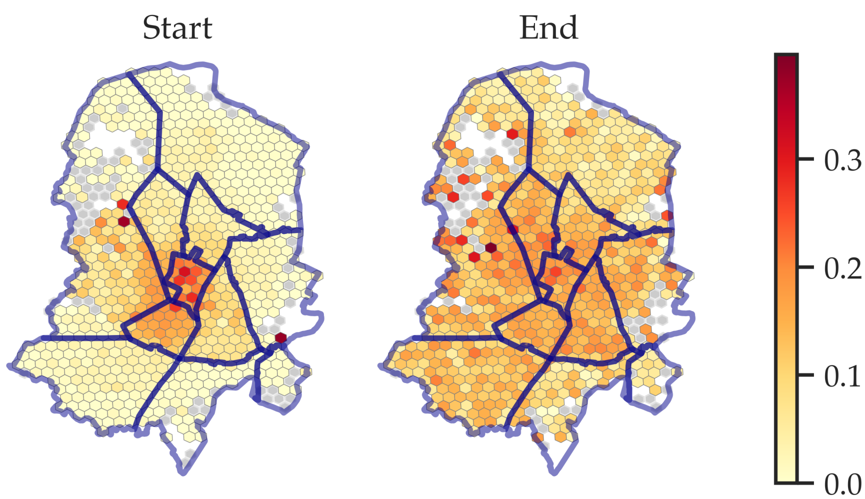

Notes: The left map shows the fraction of surged rides by trip starting location. The right map shows the fraction of surged rides by trip ending location. Hexagons that have less than 20 total rides over the sample period are not shaded (plotted in gray).

time spent driving) is relatively flat throughout the day, hovering around 30 to 35%.

Figure 4: Vacancy Rate Within Day

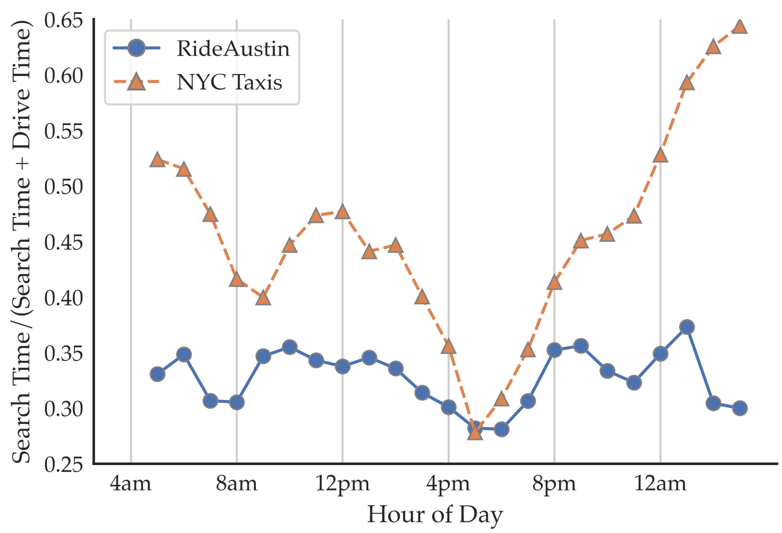

Notes: This plot shows the average ratio of search time to total driving time. Search time is equal to times between a previous ride's drop-off and the subsequent ride's dispatch. Driving time is time spent on a trip as well as driving to pick up the passenger. Data for New York City taxis is from Fréchette et al. (2019).

This figure replicates a similar statistic calculated by Fréchette et al. (2019) for New York City taxis, with the data from their analysis also plotted on the graph. We see that search is

Figure 3: Distribution of Rides and Surge Across and Within Days

(a) Frequency of Rides **(b)** Probability of Surge

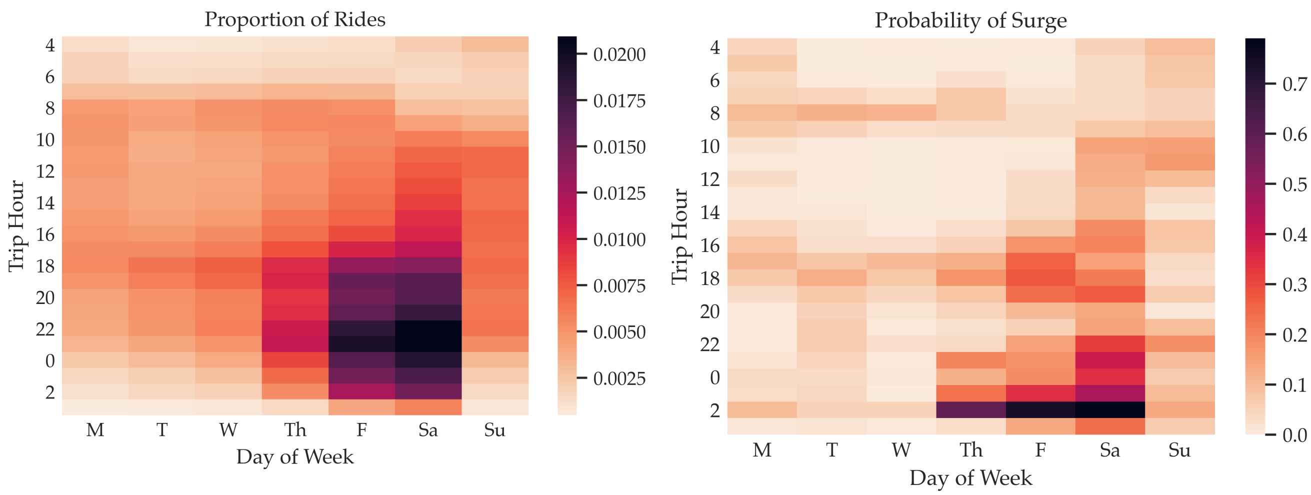

Notes: In panel (a), each cell represents the proportion of rides occurring in that day-hour relative to all rides in the sample. In panel (b), for each cell we plot the proportion of observed rides in that day-hour that are surged.

fundamentally different in ridesharing in two ways. First, the vacancy rate in ridesharing exhibits far less within-day variation. Second, the vacancy rate is lower at any time of the day. This suggests that search and match frictions are far lower in ridesharing markets, which is expected given that participants are matched using a centralized dispatcher. It also further highlights the importance of exit as ridesharing drivers can more easily exit the market rather than engage in costly search.

While match frictions are lower in ridesharing, these gains are not uniform across the city. In Figure (5), we show the mean search time for drivers based on the neighborhood of their last drop-off. We see that after completing a trip that ends in the central neighborhoods, drivers spend an average of 11 minutes searching for their next ride. In contrast, rides that end in the non-central areas require drivers to search longer until their next ride. These highlight the presence of dynamic inefficiencies. Riders do not internalize that their destination choices can result in a spatial misallocation of drivers, who must then spend more time driving in order to find their next passenger.[14] Figure (C8) in the Appendix shows that these frictions exist from the viewpoint of riders as well. In particular, riders face a longer waiting time in non-central areas relative to central areas.

[14] Brancaccio et al. (2020) refer to this inefficiency as "pooling externalities".

Table 1: Surge Frequency

Surge	Fraction of Rides		
	All	Fri.-Sat.	Sun.-Thurs.
1.00	86.02	77.31	93.6
1.25	5.32	7.77	3.18
1.50	4.17	6.76	1.91
1.75	1.5	2.59	0.56
2.00	0.96	1.65	0.35
2.25	0.31	0.59	0.07
2.50	0.47	0.88	0.12
2.75	0.22	0.43	0.04
≥3.00	1.03	2.03	0.16
N	1,403,783	653,025	750,758

3.3 Evidence of Strategic Search, Entry, and Exit Decisions for Drivers

Finally we highlight the various factors that influence the strategic decisions of drivers. In particular we show that drivers strategically target high demand areas and that they tend to "chase" the surge.

3.3.1 Entry

Drivers in our data average only 3-6 rides per day over our sample period (this translates to working for about one hour). However, the actual workload varies each day with the modal number of trips being 1 ride per day. Figure (C6) shows these distributions. Unlike taxis, whose drivers tend to work longer and fixed shifts, the nature of ridesharing as being part of the gig economy necessitates a focus on entry and exit.

Figure (3a) highlights the intra-day variation in the number of rides. These patterns are also reflected in driver entry behavior. Figure (6) plots the distribution of hour of entry (i.e. what time do drivers begin working?) along with the average number of trips drivers complete given their entry hour.[15] For example, the graph shows that 6.4% of drivers enter the market at 7pm and that drivers who enter at 7pm complete an average of 5 rides. It is clear from the figure that drivers' workload peaks in the evening; correspondingly, that is also when we observe the highest rates of entry during the day. This suggests that drivers are more likely to enter the market when

[15] We cannot observe when the driver logs on or off the app (i.e. formally enters or exits the market). We assume that a driver enters the market 15 minutes before their first trip (as this is the mean time for drivers searching between trips, which we can observe). We also assume that a driver exits if we do not observe them on a trip for 60 minutes, and take the exit time as the drop-off time of their last trip. Figure (C12) shows the distribution of searching time between rides.

Figure 5: Search Time By Drop-off Location

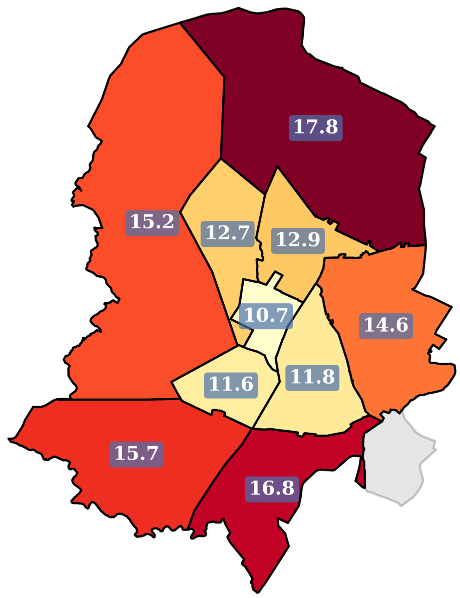

Notes: This plot shows the mean search time by neighborhood. Search time is equal to time (in minutes) between a previous ride's drop-off and the subsequent ride's dispatch. Neighborhood is the previous ride's drop-off area.

they anticipate higher earnings.

3.3.2 Search and Exit

While centralized matching reduces search frictions, the search strategy of drivers still plays an important role in determining which riders they are matched to and, consequently, their earnings. A driver's search strategy will be affected by their expectations of earnings for each location and, due to travel costs, the geography of the space they search. Ideally, if we could observe drivers at all times of the day, we could see how they choose to search. However, as mentioned before, our dataset limits us to only observing when drivers are involved in a trip. Figure (7) illustrates a driver's shift and shows what we can observe. For a given trip, we can use where the driver's *previous* ride ended to know where the driver started searching from. Then, we are able to see where a driver was at the time they were assigned (i.e. dispatched) to a passenger. By comparing these coordinates (and times), we are able to infer how the driver chose to search for their next ride. For example, in Figure (7), this strategy would correspond to comparing the coordinates of D_2 to the coordinates of E_1.[16] The key insight is that the dispatch coordinates give us a snapshot of where the driver was on their search path at the time they were assigned to their next ride.

[16]In Figure (7), the driver searches three times during their shift. However, only the search that occurs between two trips is used in this analysis, as it is the only one where we observe the start and end.

Figure 6: Entry and Rides Within Day (Fridays and Saturdays)

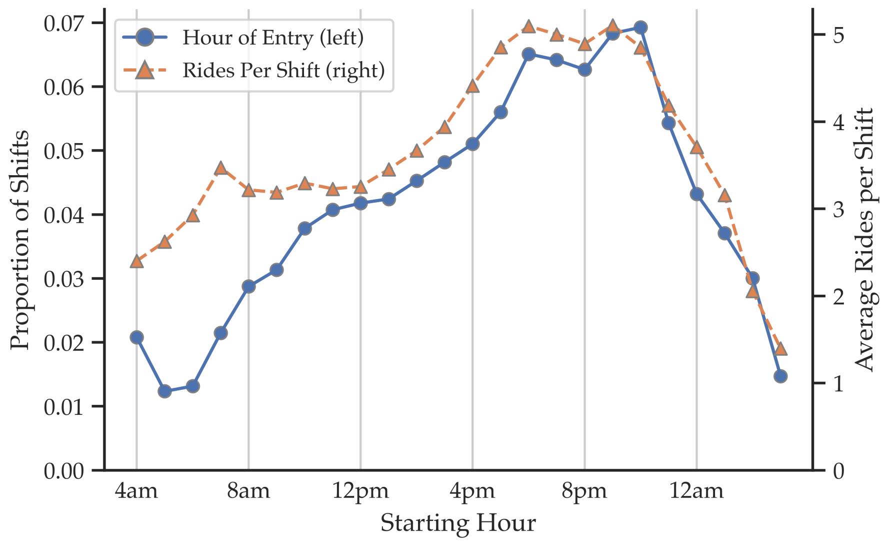

Figure 7: Example Driver's Shift

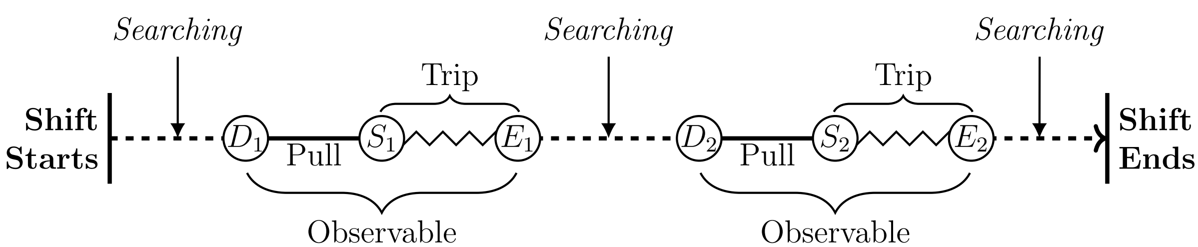

Notes: The diagram shows a driver with two rides during their shift. D_i, S_i, and E_i are the dispatch, start, and end times for trip i. These three times (and the corresponding coordinates) are observable in our dataset.

To identify the drivers' search strategy, we would ideally assign randomly a driver to a location on the map and observe how they search starting from their assigned spot. As drivers do not know the destination of the trip prior to accepting their assignment, the drop-off locations provide a close analog to this experiment. For a given neighborhood where a drop-off occurs, we calculate the average coordinate of the driver's *subsequent* dispatch location. We do this for different bins of search time (the time between the driver's drop-off and their next dispatch). By piecing together these individual snapshots, we are able to trace out the average search path for drivers based on their start location. This is shown in Figure (8). We can see that as drivers have more time to search, they aim to get closer to the downtown area, which is both where most rides occur and is the most central location. This suggests that drivers are indeed strategic in their search and that there are some commonly held strategies across all drivers.

Another implication of Figure (8) is that drivers perceive the outer suburban areas to have low earnings potential (since they do not spend time searching there). We should then expect higher

Figure 8: Search Path by Drop-off Location (Fridays and Saturdays)

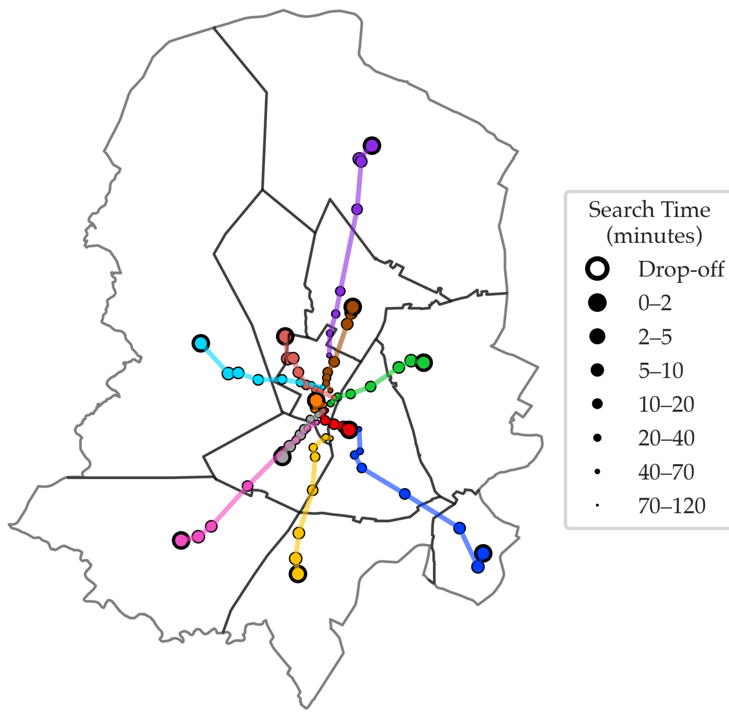

rates of exits in these areas, i.e. when a driver completes a trip in a non-central area, we would expect that they would be less likely to continue working. As Figure (C9) shows, this is exactly what we find in the data. Table (C8) supplements this by showing exit rates of different regions broken down by the start location of the trip. Regardless of where the trip began, exit is more likely the further the drop-off location is to the city center. This highlights the spatial nature of drivers' labor supply decisions.

Finally, we also find that drivers target areas where they expect higher earnings, in particular, that drivers appear to be "chasing the surge". If drivers are targeting particular areas, then we should expect the distance that they are "pulled" to meet their assigned rider to be smaller.[17] In Figure (9), we plot the average pull distance (how far a driver travels from their dispatch location to the trip's start location) relative to how much time the driver had to search since their previous trip was completed. This is important as drivers who get dispatched to their next ride soon after dropping off a passenger will not have enough time to strategically search.[18] We calculate this under two scenarios: if the ride they are dispatched to is surged and if it unsurged. The patterns observed in this figure allow us to estimate how much of the driver behavior in our model is

[17] In Figure (7), this is travel from D_i to E_i.

[18] Using the example in Figure (7), this would be plotting the distance from D_2 to S_2 on the y-axis and the difference in time from E_1 to D_2 on the x-axis.

Figure 9: Pull Distance by Search Time

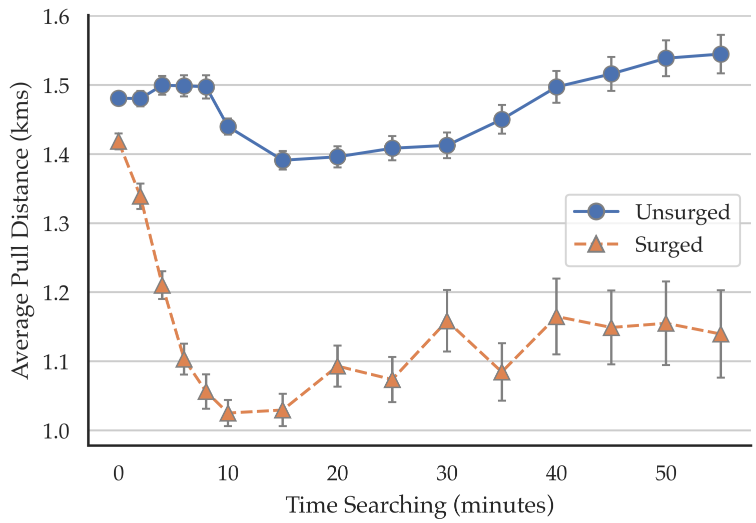

explained by continuation values of strategically searching in different locations.

We find that drivers are generally pulled from fairly short distances, with average distances ranging from 1 to 1.5 kilometers. However, it is difficult for drivers to perfectly predict where demand is going to occur (otherwise the pull distance would have been close to zero). We also see that the pull distance for rides soon after drop-off ($\leq$ 2 minutes) are generally longer than when the driver has more time to search. Lastly, when the subsequent ride is surged, drivers have much lower pull distances that fall rapidly in the first 10 minutes of search time. This evidence is consistent with drivers chasing the surge (if they have enough time). It also suggests that surge plays a role in helping drivers know where to target their search efforts.[19]

3.4 Takeaways

In our model of supply, the key parameters to be estimated will be the variances of idiosyncratic shocks relating to searching different locations, exiting, and entering, as well as the value of the driver's outside option. The patterns we find in the data shed insights into how we aim to identify the parameters.

The driver's observed search strategy determines the relative importance of location fundamentals and idiosyncratic shocks. Figure (8) shows that, regardless of their starting locations, drivers exhibit a similar strategy of aiming to reach the same location: downtown Austin. As Figures (1) and (2) show, this is also the location of the highest demand and the highest rates of surged rides. Similarly, Figure (9) also shows that drivers try to position themselves closer to surged rides. These statistics suggest that drivers are incentivized by higher fares, and that their

[19] Like Uber, drivers for RideAustin are notified on the app which areas are currently experiencing surge pricing.

search is targeted at earning these higher fares.

As we illustrate in Figure (7), a data challenge we face is that we do not observe what drivers do outside of a trip. In our estimation, we leverage that the dispatch location and time provides a snapshot of the driver's search activity. First, the pull distance (difference between dispatch and pick-up locations) tells us how close the driver was to the rider. This logic, which we use to interpret Figure (9), highlights that the pull distance can be used as a measure of how strategic drivers are. Second, in Figure (8), we observe how drivers behave when they have more time to search. If drivers have longer search times, this implies that their search is less strategic, i.e. not targeted towards finding passengers.

Finally, we observe that drivers tend to complete only a few rides per day. We therefore develop a model that incorporates entry and exit of drivers. The entry and exit rates will be informative in identifying the outside option parameter, as this will show whether drivers prefer to engage in ridesharing over their alternate activity. Figure (6) shows that drivers are more likely to enter at higher activity times of the day and therefore when they expect higher earnings. Figure (C9) shows that there is spatial variation in the exit rates of drivers; in particular, we see higher exits if they are forced to take riders to low-value areas. In our model, the geographical variation in the entry of drivers will also be used to understand how much of the entry behavior we observe is driven by model fundamentals versus driven by unobservables.

4 Model

Our model incorporates four key features of ridesharing markets: (1) demand for rides that depends on price and waiting time; (2) supply of drivers where drivers strategically choose to search, enter, or exit; (3) a matching algorithm; and (4) a surge pricing algorithm. We adapt Buchholz (2020)'s model of the taxi market to account for the specificities of the ridesharing market.

In the demand side of our model, at every point in time, riders (r) in every location i open the app and decide whether or not to request a ride after observing the price and expected waiting time. On the supply side, drivers who have already decided to enter are assigned to riders to drop them off to their desired locations; if they are unassigned, they can then choose to search the city (by driving to a different location) or exit the market. Drivers currently not in the market choose whether or not to enter the market. Additionally, our model has a matching technology that assigns drivers to riders. This technology approximates a "first-dispatch protocol" that RideAustin uses, where the rider is assigned to the nearest available driver. Finally, our model includes an endogenous surge multiplier that is observable by all agents. In the following sections, we outline each of these parts of our model in more detail.

We assume that the city is a network of L locations given by $\mathcal{J} = \{1, 2, \ldots, L\}$. As we are analyzing the ridesharing market within a day, we assume that time is discrete and that the time horizon is finite i.e. $t \in \{1, 2, \ldots, T\}$. The distance between any two locations i and j is denoted by δ_{ij} and the time taken to travel between locations is given by τ_{ij}. There are two types of agents in the market: riders (r) and drivers (v). At a location i in time t, there are r_i^t riders who request a ride and v_i^t drivers. We denote the vector of riders and drivers in locations across the city at time t as $\boldsymbol{r}^t$ and $\boldsymbol{v}^t$, respectively.

4.1 Demand for Rides

In our model, an exogenous pool of potential riders O_i^t open the app and observe the price (surge factor) and expected waiting time (time for a driver to arrive at the pick-up location). Based on these factors, some customers will choose to request a ride. Among those who request, if a rider is matched to a driver, they will be picked up and have their trip completed. If a rider is unmatched, then with some probability they will re-request in the next period, or otherwise exit the market.

To implement this, we assume a reduced form stochastic demand model in each location-time cell. This results in a realized demand after observing the base price for a given origin-destination pair. We assume demand is of the form:

$$\log\left(\tilde{r}_i^t\right) = \alpha_i^t + \theta_1 \log s_i^t + \theta_2 \log w_i^t + \theta_3 \log O_i^t + \varepsilon_i^t \tag{1}$$

where $\tilde{r}_i^t$ is the number of new riders requesting in location i at time t, s_i^t is the surge factor, and w_i^t is the average waiting time. O_i^t is the number of people opening the app, and represents the (exogenous) potential pool of riders.

From the $\tilde{r}_i^t$ people who request rides, the app will match as many of them as possible to vacant drivers (this process will be described in the next section). Those who do not have their requests fulfilled will either exit the market (with probability ϖ) or request again in $t+1$ (with probability $1-\varpi$). If they request again in $t+1$ and still find themselves without a match, they will either exit the market or request again in $t+2$, with the same probabilities as before. This process repeats until a maximum waiting period of G. This means that at time t there will be riders who initially requested their ride in periods $t-G$ to $t-1$. We will denote the number of re-requesters as $\overline{r}_i^t$. Therefore, the total number of requested rides in location i at time t, denoted as r_i^t, is the sum of $\tilde{r}_i^t$ (new requests) and $\overline{r}_i^t$ (re-requesters).

4.2 Matching

Ridesharing platforms act as a centralized dispatcher who assigns available drivers to customers requesting a ride. In a traditional taxi market, e.g. as studied by Buchholz (2020), drivers and riders must be in the same location to be able to find each other and create a match. However, ridesharing apps allow for matching of drivers and riders who are in completely different locations.

In this section, we describe the matching algorithm to assign riders to drivers. We develop an algorithm that approximates a "first-dispatch protocol" wherein riders are matched to nearest available driver (Yan et al., 2019). We show in Appendix D.1 that the patterns we observe in the data justify this approach.

As denoted above, the vectors $\boldsymbol{r}^t$ and $\boldsymbol{v}^t$ capture the number of riders and drivers, respectively, in locations across the city. The matching algorithm $m(\cdot, \cdot)$ takes in as inputs the vector of riders and drivers $(\boldsymbol{r}^t, \boldsymbol{v}^t)$ and outputs a square matrix $\boldsymbol{P}$ of "pull probabilities" from each location to every other location. Each entry p_{ij} is the probability that a driver in location i is matched (or "pulled") to a rider in location j.

$$\boldsymbol{P}^t = m\left(\left\{r_1^t, \ldots, r_L^t\right\}, \left\{v_1^t, \ldots, v_L^t\right\}\right) \tag{2}$$

The matching algorithm focuses on pulling drivers to the locations where they are needed. Within a location, we randomly assign drivers to riders. However, we give priority to riders who have waited longer (i.e. we first assign drivers to riders who have waited G periods, then $G-1$, and so on).

Next, we show how we recover the $\boldsymbol{P}$ matrix and properties of the matching algorithm via simulations.

4.2.1 Implementing the Algorithm

Recall that we have divided the city of Austin into equally sized hexagons (Figure A1). Each of these hexagons correspond to a location i in our model. For each hexagon i, we define its local neighborhoods as follows. We denote the six adjacent hexagons as Ring 1 of that hexagon i. The 12 hexagons adjacent to the Ring 1 hexagons are known as Ring 2, and so on. This can be seen in Figure (10) where we show the different rings of a single hexagon. While this figure denotes this for just one hexagon in the city, we create these "rings" for every hexagon in our grid. This means that for any two hexagons $i, j \in \mathcal{J}$, we can calculate their ring relationship $Ring(i,j) = Ring(j,i) \in \mathbb{Z}_{\geq 0}$.

Next, to obtain the matrix $\boldsymbol{P}$, we use a matching algorithm that emulates the first-dispatch protocol. There are two aspects to the matching algorithm. First, it is frictionless: if a driver is matched to a rider by the central dispatcher, the match will occur and the trip will be completed with certainty. This is akin to a Leontief matching function. Second, it involves stages of pulling in drivers. To give more detail, in each location i, the algorithm initially matches as many drivers to riders who are both in that location ($\min\{r_i^t, v_i^t\}$). After this step, locations will either have excess

Figure 10: Hexagon System

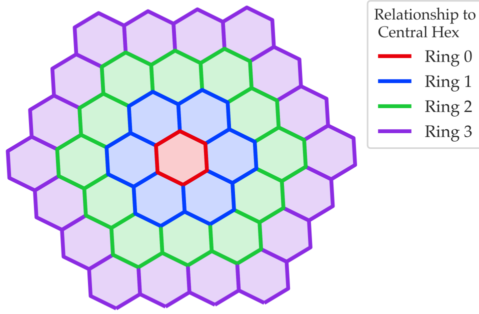

demand (unmatched riders) or excess supply (vacant drivers) or neither. Next, the algorithm takes all locations i that still have excess demand and matches riders in i randomly to vacant drivers in j, where j is a location in Ring 1 of i. After this, excess demand and supply counts update and the process repeats with Ring 2. We continue the process until excess demand is satisfied everywhere or supply runs out.[20] Pulling individual drivers involves an element of randomness, so the matching algorithm is a stochastic process. For a given distribution of riders and drivers $(\boldsymbol{r}^t, \boldsymbol{v}^t)$, we average observed matches from simulations of the matching algorithm to calculate the pull matrix $\boldsymbol{P}$.[21]

4.2.2 Properties of the Matching Algorithm

In this section, we examine some properties of our simulated matching function. First we show that as the market thickness increases, matching becomes more efficient.[22] Second, we show that drivers in our data seem to be strategically choosing where to locate themselves. To do this, we simulate how the outcome of the matching algorithm changes as the market becomes thicker. In each of our simulations, we keep the ratio of riders to drivers the same, i.e. we scale up demand and supply proportionately.

In Figure (11) on the x-axis, we plot total demand across the city while simultaneously increasing supply so that the resulting is ratio fixed at one-third. On the y-axis, we plot the average pull distance as a result of the matching. We consider three different distributions of total demand and total supply. First, we distribute demand and supply across locations as we observe in the

[20]See **??** in the Appendix for an illustration of this process.

[21]This matching function differs from that in Castillo (2019) in several ways. His matching function *sequentially* matches riders to the closest driver according a random order, while ours function matches *simultaneously* at a city-wide level. This means that our matching reduces the possibility of mismatch (i.e. that a driver could have instead been assigned to a closer rider). In addition, we are able to generate explicit pull probabilities, which can explicitly enter the driver's value function.

[22]Market thickness is captured by the number of agents in the market (i.e. given the fixed geography, an increase in the number of agents results in a denser market).

Figure 11: Matching Function Properties

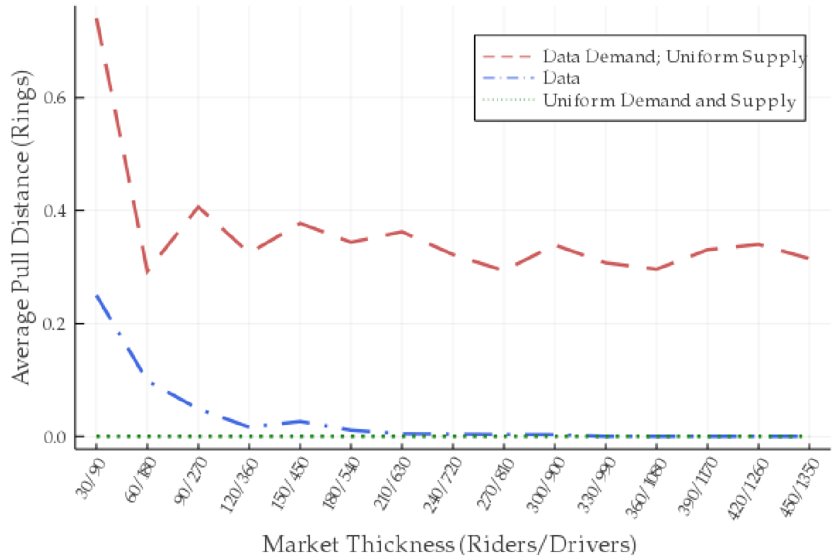

Notes: The graph shows three simulations where the distribution of riders (demand) and drivers (supply) are varied. The red line distributes demand according to the empirical probabilities for each hexagon, while supply is distributed uniformly across the hexagons. The blue line uses the empirical distribution for both demand and supply. The green line distributes both demand and supply uniformly.

data. Second, we consider a uniform distribution of demand and supply over locations. Finally, we consider a scenario where demand is distributed as observed in the data, but supply is distributed uniformly.

We see that as market thickness increases, the matches that occur are more likely to involve lower pulling distances. This is expected as a thicker market increases the chance to find a driver closer to the rider's location. However, the spatial distribution of riders and drivers is also an important determinant in the efficiency of the matching algorithm, i.e. the average pull distance of drivers. When demand and supply are equally distributed across space, the matching algorithm is most efficient. As the demand-to-supply ratio is below 1, all demand will (in expectation) be satisfied by supply in the same location. Matching is least efficient when demand is distributed as in the data, but supply is distributed uniformly across space. In this situation, even as the market thickness increases, the matching is never fully efficient as the pull distance remains above zero. This is driven by areas of high demand that continue to have excess demand even as the market gets thicker. The case when drivers and riders are distributed as in the data falls in between the two prior scenarios. This is consistent with drivers strategically searching in areas with high demand. It also shows how difficult it is to perfectly predict demand since the matching is not as efficient as in the case of uniformly distributed demand and supply. However, as the market becomes thicker, the difference between the empirically and uniformly distributed cases vanishes.

In a sufficiently thick market, even if an individual driver mis-strategizes where to search, we should not expect this to have any aggregate efficiency implications.

4.3 Supply of Rides

We model the supply side of this market with drivers dynamically deciding entry, search, and exit decisions. Drivers decide whether to enter the market and thus make themselves available for trips. Once in the market, they can search around the city. If a driver gets matched to a rider, they first go to pick up the rider, then complete the trip and receive the trip's fare. If they are unmatched, they can continue searching or exit the market. We first define the payoffs from completing a single trip from location k to j. Then, we describe our model of search and exit followed by our model of entry. To contrast it to the previous literature, our supply side model extends Buchholz (2020) to account for surge pricing, centralized matching, as well as allowing for drivers to enter, exit, and search across locations.

4.3.1 Payoff per Trip

In this section, we outline how the trip fare is calculated. A trip at time t is defined as a rider in location k wanting to go to j who has been matched to a driver currently in i. We set the trip fare using the same formula used by RideAustin. The fare that a driver gets depends on the flag-drop fare b, the distance-based fare π_δ, the distance between the pick-up and drop-off locations denoted by δ_{kj}, the time-based fare π_τ, the travel time between the pick-up and drop-off locations denoted by τ_{kj}, and the surge factor s_k^t applicable for that trip (which varies with the origin location k and request time t). The total revenue that a driver earns from the trip as defined above is $(b + \pi_\delta \delta_{kj} + \pi_\tau \tau_{kj})\, s_{kt}$.[23] The costs incurred by the driver involves fuel costs in driving from i to pick up the rider in k, denoted by c_{ik} as well as the fuel costs involved in dropping off the rider in j (c_{jk}).[24] The net payoff per ride for a driver is therefore:

$$\Pi_{ikj} = (b + \pi_\delta \delta_{kj} + \pi_\tau \tau_{kj})\, s_k^t - c_{ik} - c_{kj} \tag{3}$$

[23]RideAustin additionally ensures that the minimum fare is \$5, which we also impose in the estimation. Per the company's policy, the driver keeps the entire fare from the trip net of a flat \$0.99 fee. For ease of notation, we omit this in our model.

[24]This payoff follows the structure of Buchholz (2020), who sets the fuel cost at 12.4 cents per mile for New York City taxis. Castillo (2019) sets driving costs for Uber drivers at 26 cents per mile, though this includes fuel as well as maintenance, repairs, and depreciation.

4.3.2 Search and Exit

In this section, we focus on drivers who are already in the market. Drivers who have already entered the market can either be *vacant* (available for matching) or *in transit* (engaged in a trip). We denote the state variables for a driver w who has already chosen to enter in location i at time t as $x_w^t = (l_w^t, e_w^t, \mathcal{S}^t)$, where l_w^t is the location of driver w at time t, e_w^t is an indicator for whether driver w at time t is on a trip, and $\mathcal{S}^t$ is the spatial distribution of demand and vacant drivers at t. This is defined as $\mathcal{S}^t = \{v_i^t, r_i^t\}_{i \in \mathcal{J}}$, where v_i^t is the number of vacant drivers in location i and r_i^t is the total demand at location i. Drivers who are in transit ($e_w^t = 1$) have no decisions to make until their current trip is complete. Therefore, to model the decisions of drivers, we only need to focus on vacant drivers ($e_w^t = 0$).

Vacant drivers must decide which location to drive to (search) or to stop working (exit). The set of locations that they can choose to search from is denoted by $\mathcal{A}(i)$. This decision is based on their current location (l_w^t) as well the distribution of demand and other vacant drivers ($\mathcal{S}^t$). Drivers will search by driving to the location that provides them the highest value. The value of a location for a vacant driver can be broken up into two sources.

1. With some probability, the driver gets dispatched from that location to a trip. The driver then drives to pick up the passenger and drops them off in their destination, thus receiving the trip fare. Then they continue as a vacant driver from the drop-off location.

2. Alternatively, the driver remains unmatched and can choose a new location to search (the set of available locations denoted by $\mathcal{A}(i)$) or they can choose to exit.

Given the spatial distribution of drivers and riders, $\mathcal{S}^t$, the *ex-ante* value for each vacant driver in location i at time t is given by:[25]

$$V_i^t\left(\mathcal{S}^t\right) = \mathbb{E}_{\mathcal{S}|\mathcal{S}^t}\Bigg[\sum_{k \in \mathcal{J}} p_{ik}^t \sum_{j \in \mathcal{J}} M_{kj}^t \left(\Pi_{ikj} + V_j^{t+\tau_{ikj}}\left(\mathcal{S}^{t+\tau_{ikj}}\right)\right) + \left(1 - \sum_{k \in \mathcal{J}} p_{ik}^t\right) \mathbb{E}_\varepsilon\left[\max_{j \in A(i) \cup e}\left\{V_j^{t+\tau_{ij}}\left(\mathcal{S}^{t+\tau_{ij}}\right) - c_{ij} + \varepsilon_{ij}\right\}\right]\Bigg] \tag{4}$$

The first part of the value function captures the value for a driver located in i if they are matched by the platform to a rider traveling from k to j. p_{ik}^t is the probability that a driver in location i will be pulled in to location k which is derived from the matching function described in the previous section.[26] M_{kj}^t is the probability that a rider in k wants to go to location j at time t.

[25] The expectation is taken over the distribution of riders and drivers in future periods.

[26] We assume that the matching function does not take into account drivers who are about to end trips in that region. Additionally, we also assume that drivers cannot be matched en-route to a location.

Π_{ikj} is the net payoff for the driver, as shown in Equation (3), of starting in location i, picking up the passenger in k, and dropping them off in j. This driver will complete their assignment at time $t+\tau_{ikj}$, where τ_{ikj} is the number of periods to go from i to k and then k to j, i.e. $\tau_{ikj} = \tau_{ik} + \tau_{kj}$. $V_j^{t+\tau_{ikj}}\left(S^{t+\tau_{ikj}}\right)$ is the continuation value of the vacant driver who is at location j at time $t+\tau_{ikj}$. By modeling it this way, drivers will not only want to locate themselves in areas which have high demand, but also in areas which have high demand in neighboring areas as well.

The second part of the equation represents the value of being unmatched, which happens with probability $\left(1 - \sum_{k \in \mathcal{J}} p_{ik}^t\right)$. If this happens, a driver can choose to search in any of the locations accessible to them or can choose to exit. $\mathcal{A}(i)$ is the set of all locations in $\mathcal{J}$ accessible from i and e is the option to exit the market. Driving to location j from location i incurs a fuel cost c_{ij} and takes time τ_{ij}. $V_j^{t+\tau_{ij}}\left(\mathcal{S}^{t+\tau_{ij}}\right)$ is the continuation value of the vacant driver who is at location j at time $t+\tau_{ij}$. ε_{ij} is drawn from a Type 1 Extreme Value (EV) distribution with scale parameter σ_ε. This shock captures preferences of drivers for a particular location. We assume that exiting is permanent and that the value of exiting is $V_e^t\left(\mathcal{S}^t\right) = \mu(T-t) = \mu_t$, where μ is an outside option that accumulates each period. The fuel cost and travel time for exiting are both zero, $c_{ie} = \tau_{ie} = 0$. The model for drivers is summarized in Figure (12).

The driver's problem highlights the two sources of inefficiencies present in the market. At the first step, there is a probability that a driver is matched to a rider. In Equation (4), this is represented by $\sum_{k \in \mathcal{J}} p_{ik}^t$. This represents the static inefficiency: the presence of frictions preventing riders and drivers matching from one another. As the probability of being pulled increases, this is associated with a decrease in the static inefficiency. Note that under centralized matching, $p_{ik}^t > 0$ for some $k \neq i$. Without centralized matching, we would have $p_{ik}^t = 0$ for all $k \neq i$ as drivers and riders not in the same location would not be able to find each other. If the driver does get matched, then the rider chooses the destination. This second step is what creates the dynamic inefficiency: riders do not internalize their destination choice, which may send drivers to low-value locations. In Equation (4), this is dictated by the term M_{kj}^t, which represents riders' trip preferences. While a vacant driver is able to choose their next location, an in transit driver has no choice in where the rider will take them. This means they will be forced to continue their search at a potentially suboptimal location.

At the end of each period, vacant drivers decide where to search or whether to exit the market. This means that a driver in location i solves the following problem:

$$j^* = \underset{j \in A(i) \cup e}{\operatorname{argmax}} \left\{ V_j^{t+\tau_{ij}}\left(\mathcal{S}^{t+\tau_{ij}}\right) - c_{ij} + \varepsilon_{ij} \right\} \tag{5}$$

Figure 12: Vacant Driver Valuation

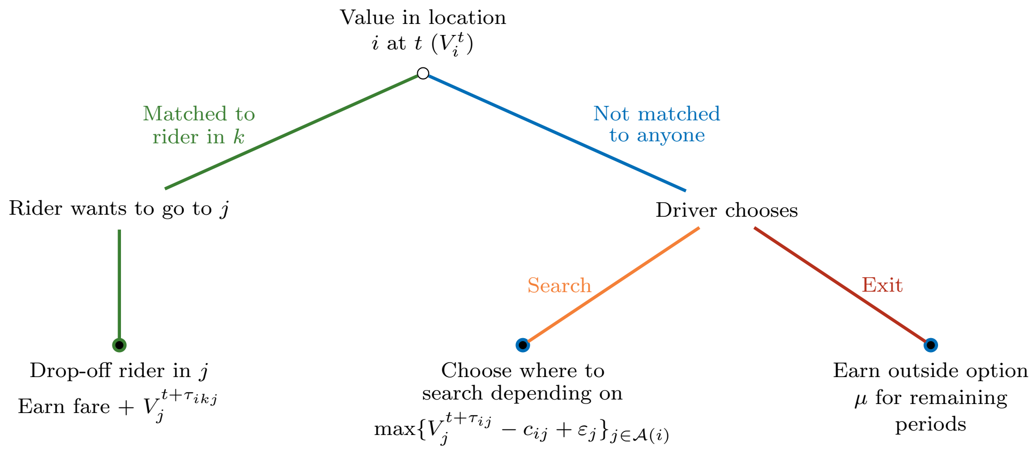

We define the *ex-ante* choice specific value function, conditional on taking action j, as:

$$W_i^t\left(j, \mathcal{S}^t\right) = \mathbb{E}_{\mathcal{S}|\mathcal{S}^t}\left[V_j^{t+\tau_{ij}}\left(\mathcal{S}^{t+\tau_{ij}}\right) - c_{ij}\right] \tag{6}$$

Given our assumption that ε_{ij} is i.i.d. Type 1 EV with scale parameter σ_ε, the probability of choosing $j \in A(i) \cup e$, before observing the draw of ε, takes a simple analytical form given by:

$$Pr_i^t\left(j\left|\mathcal{S}^t\right.\right) = \frac{\exp\left(W_i^t\left(j, \mathcal{S}^t\right)/\sigma_\varepsilon\right)}{\sum_{k\in A(i)\cup e}\exp\left(W_i^t\left(k, \mathcal{S}^t\right)/\sigma_\varepsilon\right)} \tag{7}$$

This captures the policy functions of the drivers, which we denote as $\sigma_i^t = \left\{Pr_i^t\left(j\left|\mathcal{S}^t\right.\right)_{j\in\mathcal{J}}\right\}$. Time ends at T and if a driver has chosen not to exit before then, the continuation value is set as $V_i^t = 0$ for all $i \in \mathcal{J}$ and $t > T$.

4.3.3 Entry

Next, we consider the problem of a driver deciding whether or not to enter. We assume that in time t, at each location i, an exogenous number of drivers consider entering the market, denoted as $\bar{V}_i^t$. Each potential driver decides whether to enter or not. If they enter, they immediately become available to be matched to riders. If they do not enter, they receive μ_t for the rest of day.[27] The potential driver obtains draws η_i^t from a Type 1 EV distribution with scale parameter σ_η for both options in their choice set: entering the market in location i at time t or staying out

[27] This setup restricts drivers to only one opportunity to enter the market. When estimating the model, we divide up the day into 3-hour shifts, which means that the driver is restricted to making one entry decision within a 3 hour period (however they could still enter in different shifts).

for the remainder of the day. Given this setup, the utility from entering is given by:

$$V_{i1}^{t} = V_{i}^{t}\left(\mathcal{S}^{t}\right) + \eta_{i1}^{t}$$

The utility of the driver's outside option (staying out of the market) is given by:

$$V_{i0}^{t} = \mu_{t} + \eta_{i0}^{t}$$

Therefore a driver in location i solves the following problem:

$$j^{*} = \underset{j\in\{0,1\}}{\operatorname{argmax}}\left\{V_{ij}^{t}\right\} \tag{8}$$

Given the distributional assumption on the error term, this implies that the probability with which a driver enters in location i at time t can be expressed as:

$$q_{i}^{t}\left(\mathcal{S}^{t}\right) = \frac{\exp\left(V_{i}^{t}\left(\mathcal{S}^{t}\right)/\sigma_{\eta}\right)}{\exp\left(V_{i}^{t}\left(S^{t}\right)/\sigma_{\eta}\right) + \exp\left(\mu_{t}/\sigma_{\eta}\right)} \tag{9}$$

4.4 Surge Pricing Algorithm

The final piece of the model is surge pricing. Surge pricing is a vector of prices for each location-time, that are a function of local market conditions. To implement this, we need to specify how surge prices are set. While RideAustin's exact pricing algorithm is unknown to us, the company provided us with all the data which serves as an input into their surge pricing algorithm. Moreover, through conversations with company representatives, we understand that RideAustin uses some function of demand and supply at each time and location to decide on the surge factor.

We use this information to approximate the company's pricing algorithm by a function $f(\cdot)$. Surge is calculated by the company at a broader geographic unit than the hexagons we have used so far. We call these units "surge areas"; they are shown in Figure (B3b). Our algorithm will produce a surge factor s_{a}^{t}, which is the surge factor in area a at 5-minute interval t.[28] As these surge areas are larger than our hexagons, we set the surge factor in the hexagons as equal to its area's surge factor, i.e. the surge factor of hexagon i is s_{a}^{t} for all $i \in a$. Further details are provided in Appendix Section D.2.

4.5 Intraday Timing

The timing of events both across periods and within periods is outlined in detail below.

[28]The spatial and temporal level at which RideAustin set surge was confirmed by company representatives.

1. At $t = 0$, there is an initial distribution of drivers and riders denoted by $\mathcal{S}^0$. This is assumed to be common knowledge among all the drivers.

2. At every time t, the following process occurs:

   (a) Vacant drivers arrive in locations, either through completing trips, searches, or entry of new drivers. This determines the vector of drivers:

   $$v^t = \left[v_1^t, v_2^t, \ldots, v_L^t\right]$$

   (b) Riders appear in each location as a function of surge in the previous period ($\tilde{r}_i^t$) along with unmatched riders from previous periods who re-request ($\overline{r}_i^t$). This determines the vector of riders:

   $$r^t\left(s^{t-1}\right) = \left[r_1^t\left(s_1^{t-1}\right), r_2^t\left(s_2^{t-1}\right), \ldots, r_L^t\left(s_L^{t-1}\right)\right]$$

   (c) Based on the distribution of drivers and riders, the matching algorithm assigns drivers to riders using the matching function:

   $$\boldsymbol{P}^t = m\left(r^t, v^t\right)$$

   (d) Matched drivers go to their pick-up locations to begin their trips.

   (e) Unmatched drivers choose a location to search or exit according to their policy functions σ^t.

   (f) Unmatched riders exit the market with probability ϖ. Those who have waited G periods exit with probability 1.

3. Drop-offs, search strategies, and driver entry decisions determine where drivers will be in the next period. This, along with the re-requesting riders, will determine next period's distribution$\mathcal{S}^1$.

4. This process continues until the end of the day $\mathcal{S}^T$ is reached.

We present a more detailed discussion of the intraday state transition and equilibrium in Appendix D.

5 Estimation

The key parameters to estimate in this model are σ_ε (the standard deviation of the idiosyncratic shock in driver's search/exit problem; Equation 4), σ_η (the standard deviation of the idiosyncratic shock in driver's entry problem; Equation 9), and μ (the value of the per-period outside option).

This section is divided into three parts. First, we discuss how we prepare our data for estimation. Second, we discuss the objects that are directly identified from the data. Finally, we discuss how we identify the remaining parameters. To compute the equilibrium, we follow a two-step procedure, where we first non-parametrically estimate many parameters directly from the data. After this, we solve the driver's dynamic optimization problems up to the unknown parameters σ_ε, σ_η, and μ. In an outer loop, we then find the parameters values that best match model moments to data moments.

5.1 Preparing the Data

We discretize and aggregate the data in space and time. We define a "day" as finite set of discrete time intervals representing a 24 hour period starting at 4:00 a.m. We choose to divide the day into 5 minute intervals, which is a natural choice given that RideAustin prices their surge every 5 minutes. As referenced before, the city has been divided into hexagons. However, we make further simplifications to make our estimation computationally feasible.

We focus only on Fridays and Saturdays, as these days have the most number of rides each week and exhibit similar intra-day trip patterns. Additionally, we divide the day into four three-hour shifts from 3 p.m. to 3 a.m. the following day and estimate our model separately on each shift.[29] Using the model notation, time is given by $t \in \{1, 2, ..., T\}$, where $t = 1$ is the start of the shift (e.g. 3 p.m.), $t = T$ is three hours after the shift start time (e.g. 6 p.m.), and each t is a 5 minute interval.

In terms of space, we also take steps to simplify this further. Given that suburban areas are not dense and feature a small fraction of rides in individual hexagons, we aggregate the non-central areas into a representative hexagon to reduce the dimensionality of our state space (Figure B4a). In the end, we are left with 83 locations in the city. In Appendix B, we describe the process of creating $\mathcal{A}(i)$, the accessible areas from each location, which is visualized in Figure (B4b).

5.2 Objects Identified from Data

We can directly identify a number of objects directly by taking averages from the data.

- We can identify the consumer transition probabilities M_{ij}^t by taking the mean of the probabilities of passengers going from i to j over all data in that shift. As a result, M_{ij}^t differs across shifts, but is constant within a shift.

[29] While ridesharing drivers to not work in defined shifts, splitting the day in this way means that when driver exits, we assume they will not return the remainder of the three-hour shift. This does leave the possibility that they could return for work in a different shift, however, our model does not consider any links between shifts.

- We set the distance δ_{ij} for a trip as equal to the ring relationship between the hexagons i and j: $\delta_{ij} = Ring(i,j)$.[30] We find in the data that drivers can travel on average 2 rings in a 5 minute interval, and so we set $\tau_{ij} = \lfloor \frac{\delta_{ij}+1}{2} \rfloor$ for $\delta_{ij} > 0$ and $\tau_{ij} = 1$ for $\delta_{ij} = 0$ (i.e. in one time interval, a driver can travel 0, 1, or 2 rings; in two intervals, they can travel 3 or 4 rings etc.).

- The company policy gives us the flag drop fare as $b = 5$, the distance-based fare as $\pi_\delta = 0.99$ per mile, and the time-based fare as $\pi_\tau = 0.25$ per minute.[31]

- We parametrize the fuel cost c_{ij} as $c_{ij} = \frac{g\delta_{ij}}{MPG}$, where g is the average per-gallon price of gas in Austin (\$2.21 per gallon) and MPG is the average fuel efficiency of cars in the data. Using information about the cars' models, we calculate MPG to be 22.7. This gives us the fuel cost c as equivalent to 9.8 cents per mile.

- From the trip data, we set the time of each driver's first dispatch within a shift less 15 minutes as the driver's entry time.[32] From this, we can calculate the number of entering drivers at each t for all days in our sample. We set $\bar{V}^t$ as 90th percentile of this distribution, which captures the pool of potential drivers. $\bar{V}_i^t$ is calculated by distributing the total entrants $\bar{V}^t$ using the empirical probabilities of first dispatch locations within a shift.

- We set $G = 2$ and $\varpi = 0.5$, which corresponds to a 50% probability of unmatched riders waiting an additional 5 minutes, and riders waiting a maximum of 10 minutes.[33]

- We set the maximum ring distance from which a driver can be pulled in from to be 10 (Figure C16).

After estimating these objects from the data, we next solve the drivers' dynamic programming problem up to the parameters $(\sigma_\varepsilon, \sigma_\eta, \mu)$.

5.3 Model Estimation and Identification

In this section, we explain how we solve our model and estimate the remaining parameters after having estimated the above objects directly from the data. We first solve the drivers' problem and then in an outer loop find the parameters $(\sigma_\varepsilon, \sigma_\eta, \mu)$ to match data moments to model moments.

[30] If $i = j$, then $\delta_{ii} = 0$ unless i is an (aggregated) non-central area, then $\delta_{ii} > 0$. See Appendix B for more details.

[31] We first convert δ_{ij} into miles and τ_{ij} into minutes based on regressions from the data so that the fare components better match the data.

[32] We shift it back by 15 minutes as this is the average searching time for drivers between rides

[33] In the data, the median time a matched rider waits for their driver to arrive is 5.4 minutes. 10 minutes is the 87th percentile in the waiting distribution (Figure C11).

5.3.1 Solving for Equilibrium

The dynamic programming problem of the drivers in Equation (4) suffers from the curse of dimensionality and thus makes it impossible to solve. Hence, we follow Buchholz (2020), who builds on insights in the firm dynamics literature pioneered by Hopenhayn (1992). We leverage the fact that given the large number of drivers, in aggregate, the driver's problem boils down to a single agent problem with deterministic state transitions. Hence we only need to compute the value functions along the equilibrium path of the states $\mathcal{S}^t$ for all t. We adapt the Taxi Equilibrium Algorithm of Buchholz (2020) to solve for the equilibrium value functions. See Algorithm (1) in the Appendix for more details.

The algorithm begins with an initial guess of the state $\mathcal{S}_0^t$ and then, given the state, updates the value functions by backward induction and then uses forward simulation to generate the transition path of the states according to the value functions. We iterate until the implied state transitions and the associated value functions are mutually consistent with each other.

Figure (D19) plots the computed value functions for all the locations over time. We can see that equilibrium value functions are closely bunched together and are downward sloping as expected. One might expect perfect spatial arbitrage across locations, but that is prevented by travel costs as well as travel time between locations which leads to heterogeneity in the value functions across space. Vacant drivers prefer to locate themselves in regions with higher and more profitable demand, but locating themselves in those regions after dropping off consumers in non-central locations is costly in terms of higher fuel costs and higher travel time. In Figure (D20), we show the model's convergence for the estimated parameters. For this, for iterations $k = 1, ..., 100$ following Algorithm 1, we show how the mean difference in driver counts in each location $\left(\frac{1}{|\mathcal{J}|}\sum_{i\in\mathcal{J}} |v_{i,k}^t - v_{i,k-1}^t|\right)$ changes. On average, we find that this count varies by 2 in successive iterations, which is unlikely to result in changes in equilibrium driver behavior.

5.3.2 Estimation of Scale Parameters and the Outside Option

With the equilibrium value functions in hand, we can then use the simulated method of moments to construct model moments that we then match to data moments. The unknown parameters of the model that remain to be estimated are:

(a) the variance of the Type 1 errors of the search and exit problem (σ_ε);

(b) the variance of the Type 1 errors of the entry problem (σ_η);

(c) the per-period outside option (μ).

The two scale parameters tell us how much of the drivers' entry, exit, and search behavior is driven by model unobservables relative to observables. Large values of σ_ε imply that drivers are more likely to search uniformly across all locations, whereas a low σ_ε equilibrium implies that drivers concentrate their search in areas where the value functions are highest, i.e. in downtown Austin. Similarly, a high σ_η implies that drivers are not more likely to enter (conditional on being distributed across space) in downtown Austin relative to the outer suburbs, while a low σ_η equilibrium should imply higher entry in the high-activity downtown areas. The outside option μ can be thought of as a reduced form of the drivers' options to earn money driving for other ridesharing platforms or working their main job if driving is a part-time job. The moments we use from the data are:

1. Average pull distance of drivers picking up riders
2. Average length of time a driver is vacant between rides
3. Number of drivers who have trips
4. Exit probabilities in different regions of the city
5. Entry probabilities in different regions of the city

(1) is informative about σ_ε since a higher σ_ε implies the behavior of drivers is determined more by unobservables. This implies that the data will show less targeted searching, which in turn implies larger pull distances. For similar reasons, (2) is also informative about σ_ε since it implies more spread out drivers and longer vacant times for drivers. (3) helps in identifying the outside option μ since the number of drivers who have trips is determined by how many choose to enter and exit. (4) is also informative about the outside option μ since the exit rates in differentially valuable regions tell us about the outside option of drivers. (5) is informative about σ_η and μ since a higher σ_η implies more spread out entry of drivers and a higher μ implies relatively higher entry in downtown Austin relative to the outer suburbs.

6 Results

6.1 Demand Elasticities

We estimate a version of the reduced form demand function given in Equation (1). As our surge (s_i^t) and potential riders (O_i^t) data are only available at the surge area level, we estimate the following equation:

$$\log\left(\tilde{r}_{ad}^t\right) = \alpha_a^t + \theta_1 \log s_{ad}^t + \theta_2 \log w_{ad}^t + \theta_3 \log O_{ad}^t + \varepsilon_{ad}^t \tag{10}$$

where a is a surge area, t is a 5 minute interval, and d is a day in our sample (the unit of observation is the same as in Equation (11)). We take waiting time (w_{ad}^{t}) to be the average waiting time in minutes for the given a, d, t cell.

Estimating Equation (10) by OLS suffers from the classic endogeneity issue. To circumvent this, we need an exogenous supply shifter to causally estimate the parameters of the demand equation. We use the number of rides ending in location a as an instrument for the price (s_{ad}^{t}).[34] An increase in the number of rides ending in location a imply a positive shift in the supply of drivers in that area. This means there will be a greater number of drivers available for meeting demand in location a, which should push down the price in that location. Note that the number of trips ending in a location are not an endogenous choice of drivers, but are rather a result of riders' decisions from previous periods. This is important for the exclusion restriction to hold. It is plausible that the decision of a rider choosing to travel from another location b to location a and *arriving* at time t is orthogonal to the decision of a rider in location a *requesting* a ride at time t.

The results from the estimation are shown in Table (2). The first column shows the result from the first stage of the model. An increase in the number of rides which are completed in location a lead to a decrease in the surge factor in a. In the second column, the absolute value of the price and waiting time elasticity of demand are 1.62 and 0.014 respectively. The elasticity estimates are similar to those found in Buchholz (2020) and Buchholz et al. (2020), which study taxis in New York City and ridesharing in Prague, respectively.

Our estimates however are much higher than those found in Cohen et al. (2016) and Buchholz (2020). We believe that these results reflect a young market after the exit of Uber and Lyft. Table (E9) in the Appendix shows how these estimates vary within the day.[35] While the price elasticity of demand estimates are much higher during the day, waiting time elasticities are higher at night. This is unsurprising given that we are focusing on Fridays and Saturdays when a lot of people frequent restaurants and bars at night. We use the estimates from Table (E9) and use them as an input into the estimation of the remainder of the structural model.[36]

[34] While one may expect that waiting time is endogenous as well, we do not instrument for waiting time because we do not expect the endogeneity to be very large given the rich set of fixed effects we include. Cohen et al. (2016) follows a similar approach. Moreover, our estimates of waiting time elasticity are in line with those found by Buchholz et al. (2020). However in Appendix Table E10, we estimate the demand equation using 2 instrumental variables by using lagged ending rides as an additional instrument for waiting time. The results are similar and hence we proceed with our baseline specification.

[35] The estimates for 3 p.m.–9 p.m. are similar to the price elasticity estimates Buchholz (2020) finds for short trips (< 4 miles). Almost 60% of our rides are short trips.

[36] The parameters help us generate demand at the surge area level. We then distribute the area-level demand to the hexagon-level according to the empirical distributions we observe in our trips data.

Table 2: IV Demand Results

	First Stage	Second Stage
	Surge (Log)	(Log) Rides Requested
Surge (Log)		-1.62***
		(0.23)
# Completed Rides (Log)	-0.012***	
	(0.00)	
Wait time (Log)	0.011***	-0.014***
	(0.00)	(0.00)
# People Opening App (Log)	0.011***	0.014***
	(0.00)	(0.00)
Area× Time Interval FE	Yes	Yes
F - stat	403.09	.
Observations	80388	80388

6.2 Structural Estimation Results

The unknown parameters σ_ε, σ_η, and μ are estimated by matching the model moments to the data moments described in Section (5.3.2). The results of the matching are discussed below in Section (7.1). The estimated parameters for the four shifts are shown in Table (3). The estimates for the variance of the Type 1 errors (σ_ε and σ_η) are similar, but typically lower than those found in Buchholz (2020) and Fréchette et al. (2019). The estimate of the outside option μ generally increases through the day, from an hourly outside option of approximately \$20 per hour in the afternoon shift to \$40 per hour late at night. This implies that, unsurprisingly, the threshold for drivers logging onto the app and continue driving for the ridesharing company is higher at night than earlier in the day.[37]

6.3 Model Fit

We show that our model is able to fit both targeted and non-targeted moments well. The different shifts capture high-activity periods that also have fundamentally different spatial patterns (for example, the late night shift consists primarily of trips from downtown to the suburban areas). In the results below, we group the city's neighborhoods into three regions in terms of their centrality, with Region 1 being the downtown area and Region 3 being the outermost suburbs (Figure B5).

[37] These numbers must not be interpreted as the hourly wage that they would have earned if not driving for RideAustin. Instead, this reflects the *value* that drivers have by *not* driving for RideAustin for the hour.

Table 3: Parameter Estimates

Shift	**Time**	$\boldsymbol{\sigma_\varepsilon}$	$\boldsymbol{\mu}$	$\boldsymbol{\sigma_\eta}$
Afternoon	3 p.m. – 6 p.m.	2.79	1.64	2.93
		(0.211)	(0.110)	(0.179)
Evening	6 p.m. – 9 p.m.	1.64	2.64	1.50
		(0.307)	(0.208)	(0.257)
Night	9 p.m. – 12 p.m.	3.21	3.21	2.50
		(0.445)	(0.150)	(0.214)
Late Night	12 a.m. – 3 a.m.	1.79	3.36	3.36
		(0.269)	(0.307)	(0.315)

Notes: Parameters for each shift are estimated separately. Standard errors in parenthesis.

Table 4: Targeted Moments

	Afternoon		*Evening*		*Night*		*Late Night*	
	Data	**Model**	**Data**	**Model**	**Data**	**Model**	**Data**	**Model**
Average Pull Distance (# of hexagons)	1.92	2.07	1.83	1.97	1.51	1.90	1.26	1.70
Vacant Searching Times (5 min intervals)	5.32	7.00	3.88	5.63	3.46	7.44	3.03	5.87
Drivers With Trips	481	581	644	684	695	721	559	598
P(Entry in Region 1)	0.24	0.17	0.25	0.18	0.27	0.22	0.45	0.40
P(Entry in Region 2)	0.38	0.46	0.41	0.46	0.44	0.50	0.40	0.46
P(Exit in Region 1)	0.27	0.35	0.42	0.47	0.39	0.49	0.30	0.32
P(Exit in Region 2)	0.39	0.42	0.42	0.44	0.42	0.40	0.45	0.43

We first show how our model matches the targeted moments for all the shifts and then present results for non-targeted moments. As described in the previous section, the moments we use for estimation are: (1) average pull distance of drivers picking up riders; (2) average length of time a driver is vacant; (3) number of drivers with trips; (4) exit probabilities in different regions of the city; and (5) entry probabilities in different regions of the city. Table (4) shows our model is able to reasonably match targeted moments. Notably, drivers in our model spend longer searching than what is observed in the data. In addition, Table (F12) in the Appendix shows that our model is able to also match non-targeted moments. Our benchmark model generates a similar fraction of surged rides as in the data, but a lower number of completed trips (which helps explain the lower average earnings and longer search times). Figure (F21) shows that our baseline model matches the distribution of surge prices observed in the data closely.

7 Counterfactuals

Next, we present the results from different policy counterfactuals that allow us to disentangle the relative contributions of surge pricing and centralized matching to the efficiency gains of ridesharing. First, we show how data moments change under three counterfactual scenarios, where we remove centralized matching and surge pricing separately and simultaneously. Second, we show how varying the level of surge pricing and centralized matching affects consumer surplus, driver earnings, and platform revenue. Third, given our findings, we propose a simple change to the pricing algorithm to increase welfare. We also test the implications of alternate driver compensation schemes.

7.1 Role of Surge and Matching

We evaluate the effect of surge pricing and matching in the ridesharing market by running counterfactuals where we remove each feature from the platform. Through this exercise we are able to isolate the mechanisms by which surge and matching drive the efficiency gains of ridesharing platforms. We present the results from three counterfactuals in this subsection. First, we shut off surge pricing by fixing the surge factor to be 1 in all times and locations. The fare structure under this counterfactual is independent of local demand and supply conditions. Second, we make supply local by only allowing matches when drivers and riders are in the same location. More precisely, we allow for Leontief matching only *within* a hexagon, but do not allow drivers to be pulled from other locations to be matched to a rider. This effectively removes the centralized matching that ridesharing provides. Finally, we shut off both surge pricing and centralized matching. We call this counterfactual the "gig taxi" equilibrium as this represents a traditional taxi market that lacks surge and matching but where drivers can still enter and exit.

7.1.1 Response of Moments

When we turn off surge pricing, the number of drivers drops dramatically in the late night shift. The drivers who do enter are in high demand, which results in them having no vacant search times as they quickly get matched to their next ride after dropping off their previous passenger. Given that 47% of rides in the data are surged during the late night shift, this implies that surge is crucial in inducing driver entry. This aligns with our parameter estimates as we find that the value of the outside option (μ) is highest during this shift (Table 3). In the benchmark model, surged rides primarily occurred in the downtown area (Region 1). Consistent with this, when surge is removed, we find that drivers are more likely to enter (and less likely to exit) in the downtown area as these are the highest value locations. Despite the total number of rides decreasing, we find that the drivers who do enter earn 50% more than under the benchmark model. This is because, with fewer drivers, the number of trips per driver increases. However, with so few drivers participating in the market, more ride requests are left unmet (69% versus 3% in the benchmark). Figure (13) shows that the unmet demand occurs throughout the city, even in the central locations. In contrast to the late night results, the no surge counterfactual for the afternoon shift (3 p.m.–6 p.m.) has starkly different outcomes (Appendix F.1). In particular, removing surge has little effect on the equilibrium in the afternoon. This is expected as only 18% of rides are surged in the benchmark during that part of the day and the estimate of the outside option is lowest during that shift. This exercise shows that surge works by inducing drivers to enter, which is especially important during times when drivers highly value their outside option.

Table 5: 12 a.m. to 3 a.m. Shift - Targeted Moments

	Data	**Benchmark**	**No Surge**	**No Match**	**Gig Taxi**
Average Pull Distance	1.26	1.70	1.38	0.72	0.86
Vacant Searching Times	3.03	5.87	0.00	6.30	1.83
Drivers With Trips	559	598	86	499	62
P(Entry in Region 1)	0.45	0.40	0.50	0.47	0.58
P(Entry in Region 2)	0.40	0.46	0.47	0.38	0.34
P(Exit in Region 1)	0.30	0.32	0.23	0.37	0.27
P(Exit in Region 2)	0.45	0.43	0.36	0.49	0.61

Notes: Average Pull distance is the average ring distance between the rider and driver. Vacant Searching time is the number of time periods drivers search between rides. P(Exit/Entry in Region i) is the fraction of rides ending/starting in a region which were the last/first ride.

In contrast, when we shut off matching, drivers spend longer searching for a ride and also exit at much higher rates than our benchmark model. While drivers generally search in the right areas, the fact that they cannot exactly predict the location of demand means that unmet demand is high (36%). This results in a much lower number of completed trips and lower average earnings for drivers. This highlights the important role that centralized matching plays in balancing demand and supply across space and eliminating match frictions. In Figure (13), we see that the increase in unmet demand for this counterfactual comes almost entirely from the non-central areas. Drivers are far more likely to search in central areas over the non-central areas: central areas provide higher rides, rides that are more likely to be surged, and have lower travel costs to reach them. Moreover, drivers tend to drive shorter shifts and exit sooner without centralized matching. These results speak to how ridesharing platforms, through centralized matching, can reduce the spatial inequality in access to transport. In summary, matching solves the static inefficiency, i.e. riders and drivers being unable to match with each other due to imbalances in demand and supply in localized regions.

Table 6: 12 a.m. to 3 a.m. Shift - Non-targeted Moments

	Data	**Benchmark**	**No Surge**	**No Match**	**Gig Taxi**
Average Earnings	54.56	39.83	59.85	28.40	29.47
Surged Rides (%)	46.88	48.10	0.00	38.15	0.00
Unmet Demand (%)	–	2.86	69.25	35.91	89.04
Last Rides (%)	26.38	36.64	16.54	47.48	34.25
Average Search Distance	–	20.86	–	25.36	2.83
Number of Trips	2,075	1,632	520	1,051	181
P(Search in Region 1)	–	0.32	–	0.29	0.35
P(Search in Region 2)	–	0.65	–	0.67	0.62
P(Search in Region 3)	–	0.03	–	0.04	0.03

Notes: Average Earnings is the average revenue earned by a driver during the shift. Surged Rides is the proportion rides which are surged. Unmet Demand is the proportion of requested rides which were unmet. Last Rides is the proportion of total rides which were last rides for a driver. Average Search Distance is the ring distance between the drop-off location for trip k and dispatch location of trip $k + 1$. P(Search in Region i) refers to the proportion of total searches in Region i

Finally, we test the combined effect of surge and matching by running the "gig taxi" counterfactual. Here, we remove surge pricing and centralized matching as before but maintain the "gig economy" aspect of ridesharing by still allowing drivers to enter and exit. By removing matching, this makes it more difficult for drivers to find rides as compared to the no surge counterfactual. Consequently, this magnifies the issues of removing surge: the number of drivers and total trips falls even further, while the proportion of unmet demand increases. Unlike the no surge counterfactual, drivers do have to search for their next ride, but on average they do not have to search for a long time. In the afternoon shift, there is little difference between the no match and gig taxi counterfactuals – as before, surge plays a minimal role and so removing it does not have a large impact on the equilibrium outcome.

Figure 13: Spatial Distribution of Proportion of Unmet Demand (12 a.m.–3 a.m.)

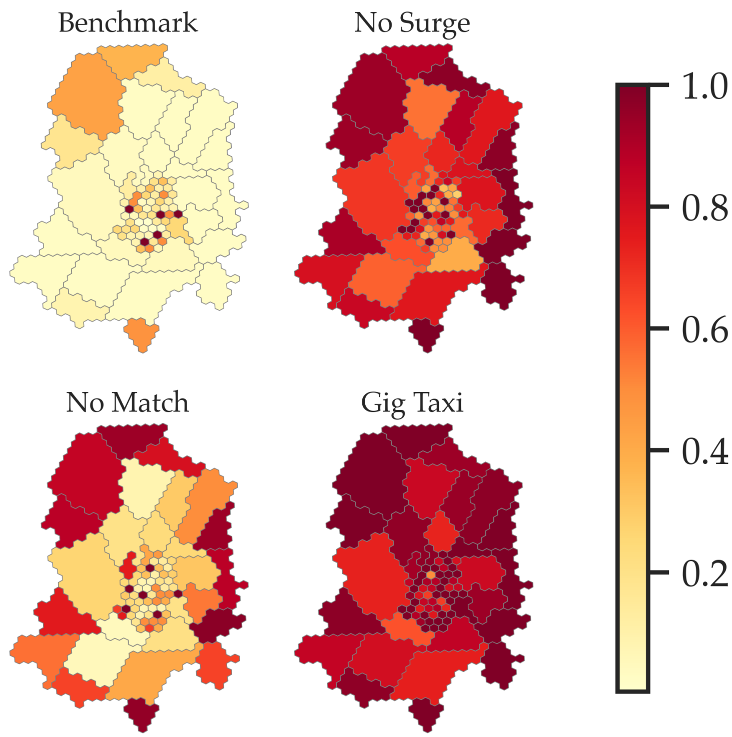

Figure 14: Comparison of Different Simulations to the Taxi Equilibrium

(a) 3 p.m. – 6 p.m. **(b)** 12 a.m. – 3 a.m.

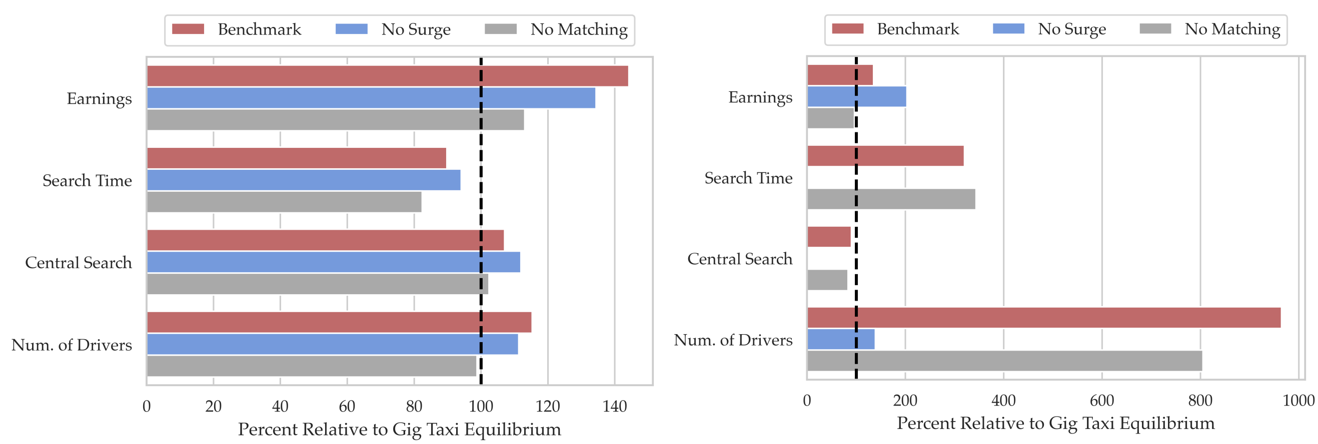

Notes: In panel (a), we show how each of the moments for our counterfactuals compares to the taxi equilibrium for the afternoon shift. In panel (b), we show this for the late night shift.

We summarize the key comparisons across the counterfactuals in Figure (14) where the black dotted line represents the gig taxi equilibrium. The red bars represent our benchmark model, the blue bars represent the counterfactual without surge pricing, while the gray bars represent the counterfactual without centralized matching. All values have been normalized to be relative to the gig taxi equilibrium. While the effects of shutting of centralized matching are consistent across the shifts, the effects of the surge counterfactual have dramatically different implications across the shifts. The results also highlight the importance of not only spatial, but also temporal variation when evaluating counterfactual outcomes.

7.2 Welfare

Given the underlying mechanisms that surge and matching play in the determining equilibrium outcomes in the model, in this section, we turn to evaluating how different counterfactual scenarios translate to changes in consumer surplus, driver revenue as well as platform profits. We then draw policy implications for regulating ridesharing platforms such as Uber and Lyft and improving the competitiveness of traditional taxis. We first define how we calculate each of these quantities. Driver revenues are defined as:

$$\text{Driver Revenues} = \sum_{v} \left[\sum_{x \in \text{Trips}} \left[\left(b + \pi_\delta \delta_x + \pi_\tau \tau_x \right) s_x - c_x \right] - \sum_{y \in \text{Pulls}} c_y - \sum_{z \in \text{Search}} c_z \right]$$

This is simply the sum of payoffs (fare less fuel cost and dollar per ride) earned on each trip x, the fuel cost for every pull y, and the fuel cost for every search z. We sum this for every driver v.

To compute consumer surplus, we use the demand function given in Equation (10) and compute the area under the curve. More precisely:

$$\text{Consumer Surplus} = \sum_{it} \left(\frac{m_{it}}{r_{it}} \right) \int_{s^*_{it}}^{\infty} \int_{w^*_{i,t}}^{\infty} e^{\alpha_{i,t}} s_{i,t}^{\theta_1} w_{i,t}^{\theta_2} O_{i,t}^{\theta_3} dw_{it} dp_{it}$$

where $\frac{m_{it}}{r_{it}}$ is the proportion of rides requested which got a ride. For implementation purposes, since these elasticities are local, evaluating consumer surplus at high values of surge and waiting time requires extrapolation (Buchholz, 2020). Hence we set the upper bound on surge and waiting time to be 7 and 30 respectively. Computing consumer surplus this way also allows us to understand the spatial heterogeneity in consumer surplus across the different counterfactuals.

Computing platform revenues is straightforward in our setting since RideAustin charges a flat $0.99 fee for each trip. Hence, platform revenues are approximately equal to the number of trips. We estimate an annual consumer surplus of $5.5 million for the afternoon shift and $44.5 million for the late night shift in our benchmark estimation.[38] Driver profits are estimated to be $4.3 and $6.9 million for the two shifts, while platform revenues are $457,000 and $601,000, respectively.

[38] This is an upper bound given that these numbers are calculated based on data for Fridays and Saturdays.

We also compute these quantities in our two main counterfactuals and compare them to the taxi equilibrium. The results are shown in Figure (15).

In the 3 p.m.–6 p.m. shift, all the models seem to generate substantial gains across the board relative to the taxi equilibrium, except for average driver revenue under the counterfactual without matching. If surge pricing is shut off, consumer surplus increases by 4.1% while driver revenues fall by 20% relative to the benchmark model. Moreover, platform revenue is unchanged.[39] However if matching is shut off, the fall in consumer surplus, driver revenues and platform revenues are substantially larger relative to the benchmark. These results are different however if we analyze the late night 12 a.m.–3 a.m. shift. Here, consumers, drivers, and the platform are all worse off relative to the benchmark under all counterfactual scenarios.

Figure 15: Comparison of Different Simulations to the Taxi Equilibrium

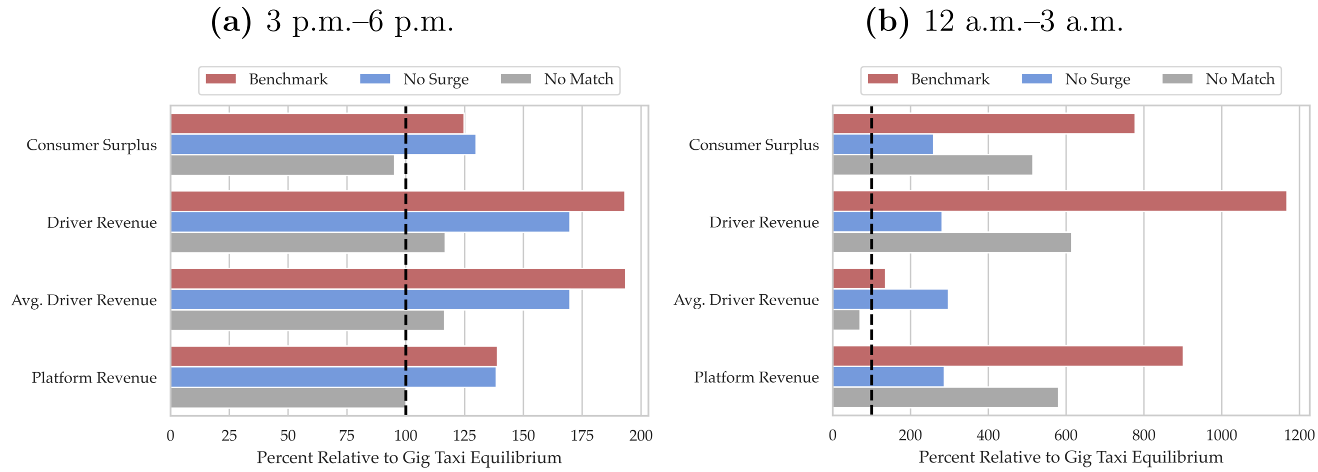

Notes: In panel (a), we show how consumer surplus, driver revenue and platform revenue for our counterfactuals compares to the taxi equilibrium for the 3 p.m–6 p.m. shift.. In panel (b), we show how consumer surplus, driver revenue and platform revenue for our counterfactuals compares to the taxi equilibrium for 12 a.m.–3 a.m. shift.

Interestingly, there is heterogeneity in the spatial distribution of consumer surplus. Figure (16) shows that consumer surplus skews towards the central areas when we shut off matching in the afternoon shift. Centralized matching is key to ensuring an equal distribution of consumer surplus across space. We see a similar spatial distribution of consumer surplus in the taxi market. These results for the late night are shown in Appendix Figure (F24). While the results there are less stark, the same general pattern appears.

Overall our results indicate that centralized matching plays a key role in the efficiency of ride-sharing through the course of the day. Surge pricing has small negative effects on consumer

[39]While economic theory predicts that flexible pricing must improve consumer surplus, this may not be as straightforward in ridesharing markets. Since surge factors are never set below one, it is not inconceivable that the downward rigidity of surge pricing may in fact not be welfare improving for consumers.

Figure 16: Spatial Distribution of Consumer Surplus (3 p.m. – 6 p.m.)

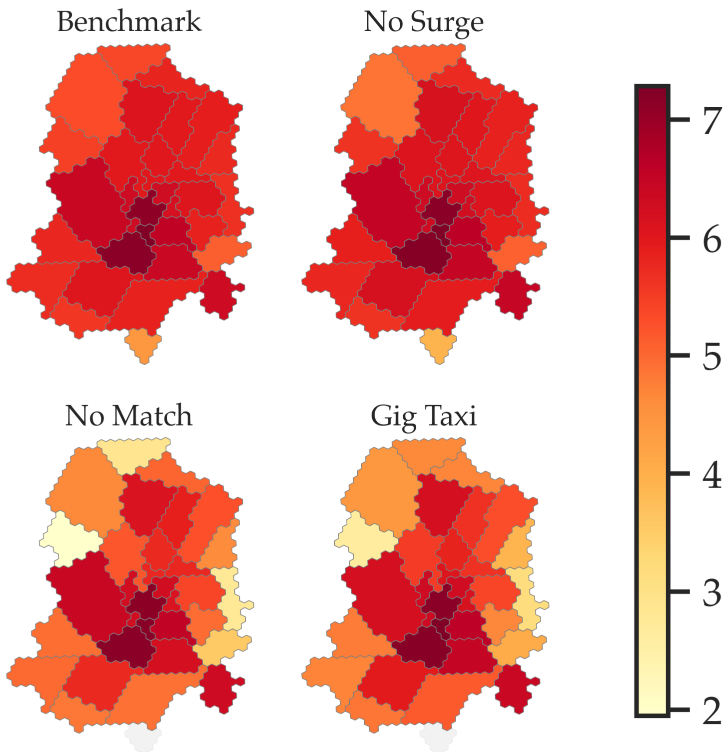

surplus in the day (relative to our benchmark model), however surge pricing plays a key role in increasing welfare late at night. In particular, during late night shifts, surge pricing and centralized matching seem to act on different dimensions and thus are likely complementary. As discussed in the previous section, surge solves the driver entry problem while centralized matching minimizes match frictions. These findings which hint at the complementarity between surge pricing and centralized matching are analyzed further in the next subsection.

7.3 Complementarity

Our model incorporates three key elements of ridesharing: surge pricing, matching technology, and flexible entry/exit by drivers. We can evaluate complementarities between these features by comparing counterfactuals where we activate each feature. This gives us 8 possible counterfactuals, whose welfare implications for the 12 a.m.–3a.m. shift are shown in Figure (F25) in the Appendix. We compare all outcomes relative to the taxi equilibrium, which has none of three ridesharing features. Consumer surplus is highest with a traditional taxi system endowed with a centralized matching technology. The intuition behind this result follows from the fact that in a traditional taxi market, supply is held fixed and therefore surge doesn't play a critical role in increasing consumer surplus. Drivers on the other hand benefit the most in a ridesharing world due to the majority of rides being surged late at night. [40]

These figures also provide evidence for complementarities between surge and matching. Moving from the flexible taxi counterfactual to the no surge counterfactual adds matching technology. Likewise, moving from the flexible taxi counterfactual to the no matching counterfactual adds surge pricing. In either case, for the 12 a.m.–3 a.m. shift, there are gains to consumer surplus, driver earnings, and platform revenues. Moving from flexible taxi to ridesharing (i.e. the benchmark model) simultaneously adds surge and matching. This change increases welfare for all agents by *more* than the sum of the gains from adding each feature separately. These results are captured in Table (7). We interpret this as evidence for the complementarity between surge and matching. To be more precise, surge pricing induces more drivers to enter and leads to a thicker market which improves the effectiveness of the matching algorithm. Appendix Section (F.3) includes further discussion of results from these counterfactuals.

Our results allow us to draw two policy implications. First, banning or capping surge pricing, as many cities are considering, may in fact harm both riders and drivers. This can be seen in Figure (F25). Second, for taxis who wish to compete with ridesharing platforms, the results show that surge pricing is not the answer. Instead, by introducing a matching technology, taxis would be able to potentially increase consumer and driver welfare. The different policy recommendations stem from the nature of supply for each of the two systems. Surge is important for inducing driver entry. As ridesharing platforms are in the gig economy, driver entry is critical to ensuring sufficient supply. In contrast, taxis with a fixed labor force do not have an entry problem, and therefore have little scope for benefiting from surge.

Table 7: 12 a.m. to 3 a.m. Shift - Complementarity

Welfare	No Surge	No Match	Benchmark	Complementarity
Consumer Surplus	159.42	414.89	677.73	103.42
Driver Revenue	181.39	514.73	1067.66	371.55
Platform Revenue	187.29	480.66	801.66	133.70

Notes: No Surge is the counterfactual without surge pricing. No Match is the counterfactual without matching technology. Benchmark is the ride sharing model (surge and matching). All figures represent welfare gains relative to the Flexible Taxi counterfactual (no surge or matching, but entry/exit as in all previous models). The fourth column represents the complementarity gain = Benchmark − (No Surge + No Match)

To further assess how these two features interact, we simulate the model by varying both features at a more granular level. For matching, we vary the maximum ring (in other words the

[40] A similar graph for the 3 p.m.–6 p.m. shift is shown in Figure (F27) in the Appendix.

Figure 17: Welfare Effects of Varying Matching and Surge

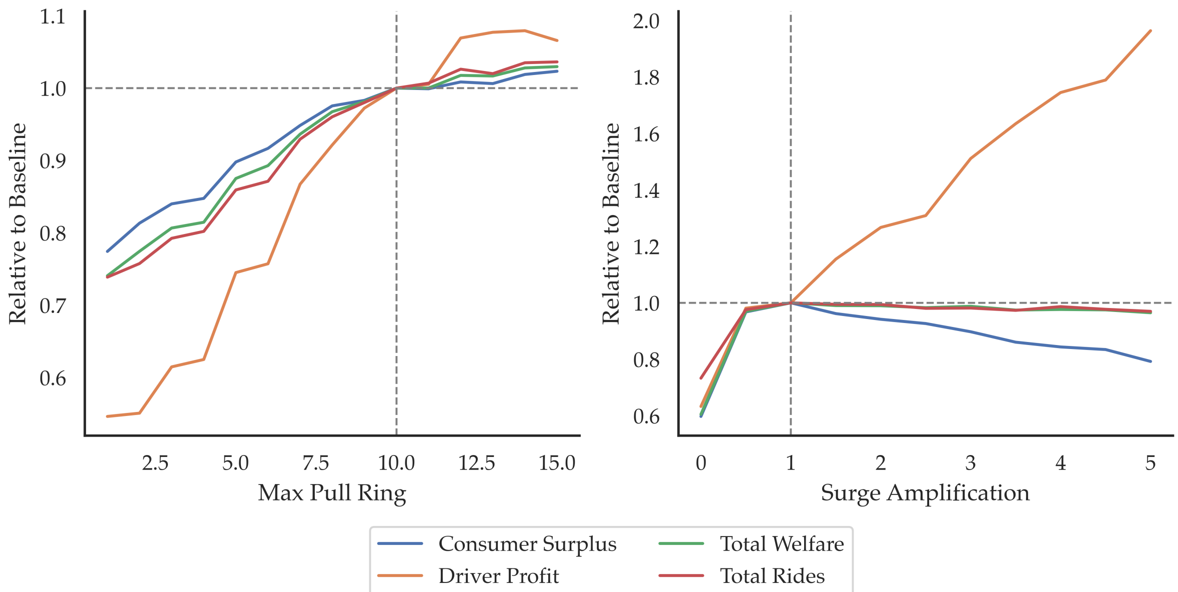

Notes: Results are simulated for each shift and then aggregated over the day. Total welfare is the sum of consumer surplus, driver profits, and platform profits.

maximum distance) from which a driver could be pulled from. The no match counterfactual only pulls from rings less than 1, while the benchmark model pulls from rings less than 10.[41] For surge, we amplify (or dampen) surge by a factor $\theta \geq 0$ such that a surge factor s becomes amplified to $s_\theta = 1 + \theta(s-1)$.[42] The no surge counterfactual has $\theta = 0$ and the benchmark has $\theta = 1$.

In Figure (17), we show the effects of varying each of these feature separately and compare the welfare effects to that of the benchmark model. In the left panel, we see that increasing the maximum pull ring (i.e. reducing match frictions) has unambiguously positive welfare effects for all agents. Unsurprisingly, there are diminishing returns to the gains from reducing match frictions, evidenced by the concavity of the benefits for all agents. In contrast, amplifying surge reduces consumer and total welfare, while only increasing drivers' profits.[43] In particular, given the other benchmark settings, the current surge is optimal for consumer welfare, but not for drivers (a result consistent with Castillo (2019)). This is because the higher surge prices out low value customers, resulting in a lower number of rides but higher overall fares.[44]

Next, we vary both features together, while keeping all other features of the ridesharing market constant. This is shown under the benchmark plots of Figure (18). These graphs plot how

[41] A maximum ring distance of 10 implies that the maximum distance from which drivers could be pulled in is approximately 9 kms.

[42] For example, a surge of 1.25 and a factor $\theta = 2$ would be amplified to $s_\theta = 1.5$.

[43] Total welfare is computed as the sum of consumer surplus, driver profit, and platform revenue.

[44] Figure (F28) shows the effects of average prices and pull distances under these simulations. In particular, a surge amplification of 5 corresponds to approximately an average price (surge factor) of 1.8.

consumer surplus, driver profits, and total welfare compare relative to our benchmark model (indicated by the yellow square). From this, we can see that while both riders and drivers view reducing match frictions as welfare increasing, there is a conflicting role for surge. Higher surge generally reduces consumer welfare but increases driver profits. By increasing both surge and the maximum pull distance, the platform would be able to increase total welfare. Moreover, the plots suggest that drivers have convex iso-profit lines for surge and matching, which supports the complementarity between the two features.

7.4 Impact of Alternate Driver Compensation and Pricing Schemes

Our results so far suggest that while matching primarily drives the efficiency gains of ridesharing, the platform's pricing structure is still key to understanding the full welfare effects. Moreover, given the unique nature of the ridesharing platform in our setting, it is not obvious how our results would apply to a scenario in the presence of more traditional driver compensation schemes as implemented by ridesharing platforms like Uber or Lyft. Therefore, in this section, we look to answer two questions. First, would these results generalize to other ridesharing companies such as Uber and Lyft? Second, are there alternative pricing structures that could increase welfare? Figure (18) shows these results. We extend the analysis from the previous section to understand how different compensation and pricing schemes change how matching and surge affect consumer surplus, driver profit, and total welfare. We run the same counterfactual simulations under two alternative policies: a platform that charges drivers a commission, and a fully flexible surge pricing algorithm.

7.4.1 Alternate Driver Compensation Schemes

The company we study, RideAustin, is a non-profit, which only takes 99 cents from every completed trip (with the rest going to the driver). A key difference between RideAustin and a platform like Uber is that Uber takes a 25% commission on rides.[45] To see whether this would affect our results, we simulate a counterfactual where the platform receives 25% of the total fare. This is shown in the second column of graphs under the header "Platform Commission" of Figure (18). We see that under this fare structure, consumers welfare and total welfare are lower in all possible combinations, as compared to the benchmark model. The platform taking a proportional cut creates a distortion which prevents it from achieving the socially optimal allocation. In particular, consumers are strictly better off if platforms did not use commission fee structure. Ridesharing platforms that use this approach do not necessarily internalize that their compensation schemes have an effect on driver payoffs, which in turn affects consumer surplus. These results however do not preclude

[45] Uber's website states "Uber charges partners 25% fee on all fares", which is also consistent with Castillo (2019).

Figure 18: Welfare Effects of Varying Matching and Surge Simultaneously

(a) Consumer Surplus

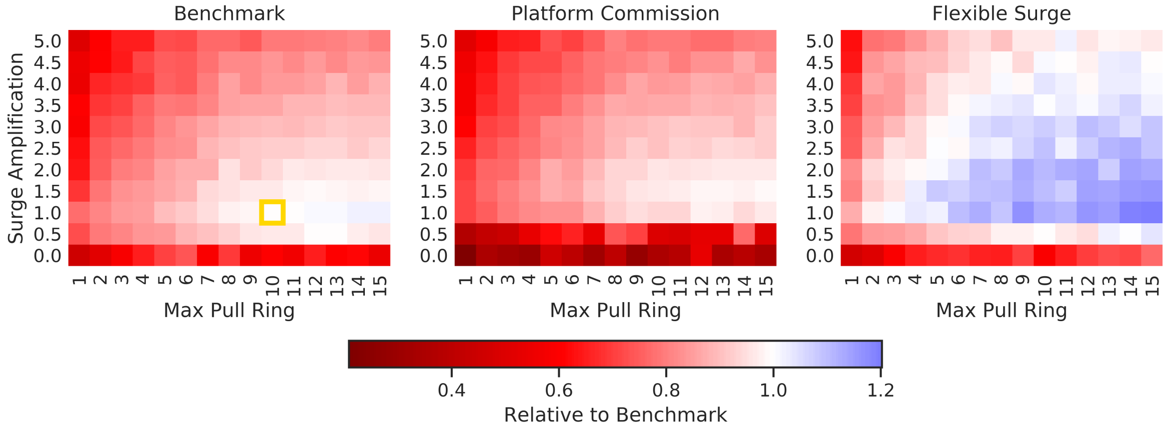

(b) Driver Profit

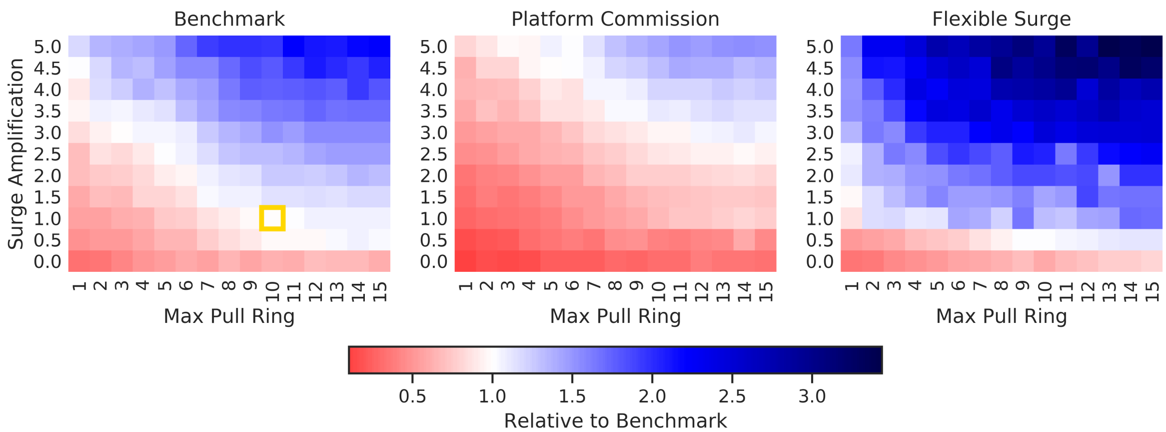

(c) Total Welfare

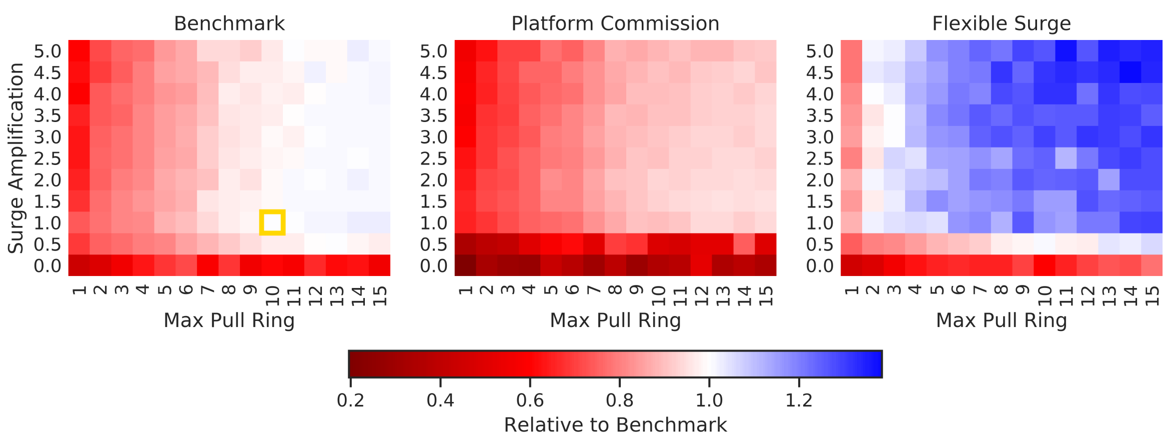

Notes: Results are simulated for each shift and then aggregated over the day. Total welfare is the sum of consumer surplus, driver profits, and platform profits. All values are relative to the benchmark model with max pull ring at 10 and surge amplification at 1 (indicated by the yellow rectangle). Benchmark indicates the baseline model that was estimated. Platform commission is a counterfactual where the platform receives 25% of the fare. Flexible surge is a counterfactual where surge is allowed to go below 1.

the existence of other compensation schemes that could achieve higher surplus for consumers and drivers relative to our benchmark model. Importantly, the general welfare differentials of surge and centralized matching continue to hold under this alternative compensation scheme. We interpret this as our results continuing to hold, even under a pay structure such as that of Uber.[46]

7.4.2 Alternate Pricing Schemes

While matching appears to be preferred by both sides of the market, there is a limitation: match frictions can only be reduced so much. In our context, the gains from pulling from a further distance diminish as eventually the entire city is covered and there are no additional areas from which to pull drivers. Selecting a different pricing structure provides many more options for the platform (or social planner) to increase welfare. Our results so far show that surge plays a more limited role in improving consumer welfare. This may be surprising given that we would expect prices that adapt to market conditions would be welfare-improving. However, one key limitation of surge, as implemented by companies like RideAustin and Uber, is that it is one-sided. The surge factor is never set below 1, which means that prices *increase* in relatively *high* demand areas, but relatively *low* demand areas do not receive a discount. Fully flexible prices should be responsive to both types of market fluctuations. This simple idea is echoed in Bimpikis et al. (2019) and Besbes et al. (2020) which study optimal pricing in ridesharing platforms. The key property characterizing optimal prices is that demand and supply are "balanced" in different locations. When drivers drop off riders in non-central locations, this results in a newly-vacant driver in an area with low demand. Consequently, this creates a mismatch in relative demand and supply at that point in time. Instead of having drivers searching their way back to high demand areas, it would be better to give a discount to these non-central locations to induce higher demand so that the driver is more easily able to find a passenger. This would ensure that supply is optimally utilized across space. To see how such a pricing rule impacts welfare, we run a counterfactual allowing for flexible surge (a surge factor that can go below 1, with a lower bound of 0.25). Our surge pricing algorithm allows us to approximate the "balancedness" property since the inputs into the algorithm are the demand and supply at a given location. The results from this exercise are shown in the third column of graphs of Figure (18). This simple change in the pricing rule greatly increases welfare for all agents as compared to the benchmark. We find evidence consistent with the market becoming more "balanced" as the time drivers spend searching between rides falls by 16.5%. Under the flexible surge structure, the trade-offs between surge and matching still persist, though the drivers' iso-profit curves appear to be more convex. This suggests that under flexible pricing, there is greater complementarity between these two features.

[46] Section F.3 in the Appendix makes this point clearer by considering a commission scheme such that drivers receive the same earnings as our benchmark model.

7.5 Static and Dynamic Inefficiencies

As argued before, transportation markets exhibit two types of inefficiencies. The first is a static inefficiency: at a given point in time, riders and drivers may be unable to match with each due to search frictions. The second is a dynamic inefficiency: drivers' location is affected by riders' destination choices, which may result in a suboptimal spatial distribution of supply. It is important to then see what role surge and matching play in reducing these inefficiencies.

We measure the static inefficiency as the proportion of rides requested which remained unfulfilled. Panel (a) of Figure (19) plots the proportion of unmet demand under different configurations. The benchmark model exhibits a small proportion of unmet demand. Drawing on the results shown before, both surge and matching play a role in clearing the market. Surge pricing solves the driver entry problem (and therefore creates a thicker market), while centralized matching helps in clearing the market. In the counterfactuals without surge or matching, the proportion of unmet demand rises to nearly 30%. The last bar in the panel shows a scenario where we shut off surge pricing and fix supply to be the median number of drivers (drivers are unable to enter or exit). This shows that with a large supply of available drivers, matching is able to solve most of the *static inefficiency* in the market. Thus both surge and matching play independent and crucial roles in mitigating the static inefficiency.

Figure 19: Static and Dynamic Inefficiencies

(a) Static Inefficiency **(b)** Dynamic Inefficiency

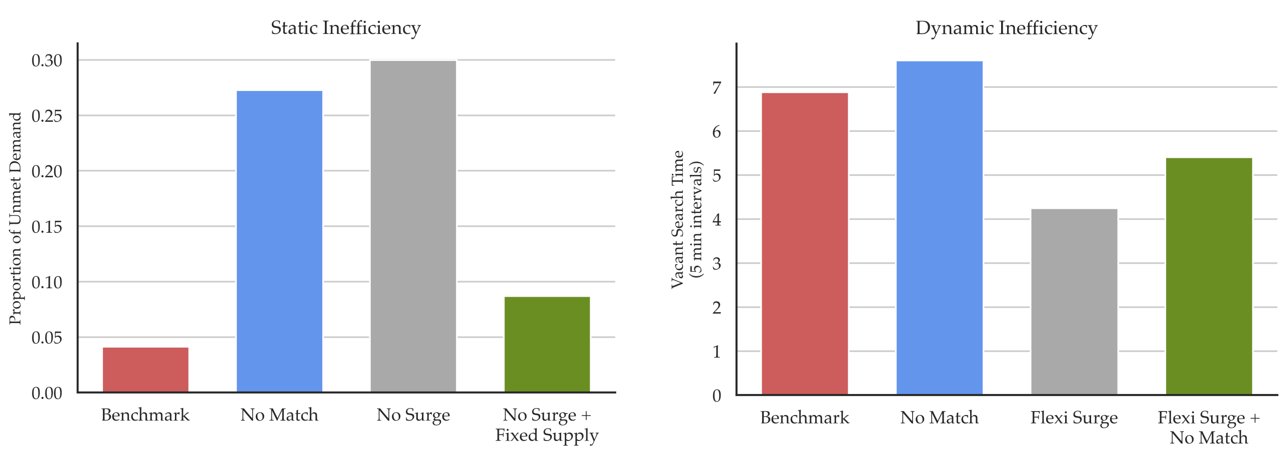

Notes: In panel (a), we show how surge and matching reduce unmet demand; our measure of static inefficiency. No Match and No Surge refer to counterfactuals without matching and pricing respectively. No Surge + Fixed Supply refers to a counterfactual without surge pricing and fixed supply of drivers. In panel (b), we show the relative importance of surge over matching in reducing the vacant time between rides for drivers. Flexi Surge refers to a counterfactual where the surge factor is allowed to go below 1. Flexi Surge + No Match refers to a counterfactual without matching but with flexible pricing.

The dynamic inefficiency is shown in Panel (b) of Figure (19) and is measured as the vacant time periods (measured in 5 minute intervals) between successive rides. Under the benchmark model, drivers wait an average of 30 minutes between rides. While there exists an option value of waiting and searching for a ride, the lower the time drivers wait between rides, the lower the dynamic inefficiency. The inefficiency here can be understood through an example: if a driver drops off a rider in the suburbs and then has to drive all the way back to downtown Austin to be matched again, this is strictly worse off compared to a situation where the driver is matched to a rider traveling from the suburbs to downtown. The benchmark surge and matching technologies are unable to address this problem. As mentioned above, the flexible pricing counterfactual conducted above aims to solve exactly that. In the counterfactual where prices are allowed to be fully flexible, we find that the vacant search time is almost halved. Thus the ability to induce demand in the suburbs and suppress demand in downtown leads to a more balanced pattern of demand and supply leading to lower wait times between rides. The last bar shows that flexible pricing is far more effective when combined with centralized matching. This is because the market still needs to be cleared even after the flexible prices lead to a balanced distribution of demand and supply.

8 Conclusion

By modeling the ridesharing market, this paper furthers our understanding of the relative importance of surge pricing and centralized matching in overcoming existing market inefficiencies. We conduct policy counterfactuals and find that both centralized matching and surge pricing are crucial in increasing consumer surplus as well as driver profits. The mechanisms through which they work, however, are different. Surge pricing improves outcomes through its effect on incentivizing driver entry, while centralized matching improves outcomes by reducing match frictions, especially in non-central areas. We also find complementarities between surge and matching, i.e. matching has a greater effect on efficiency given higher surge levels (and vice-versa). We implement a simple change in the pricing rule by making surge more flexible. This reduces spatial misallocation and therefore generates large welfare gains for all agents. Our results indicate that policymakers should be wary of banning or capping surge pricing as this may reduce consumer and driver surplus. In contrast, taxis who wish to compete with ridesharing should focus on introducing a matching technology, rather than implementing surge pricing.

Our data does not allow us to model platform competition and its impact on riders, drivers, and overall market efficiency. This is an important avenue for further research. Since for-profit platforms have been pursuing market share aggressively, it would not only require modeling their objectives in a dynamic framework but also collecting and utilizing long-term data from multiple platforms. Finally, further research should study how different pricing and compensation schemes may enhance welfare even beyond the simple changes we simulated in this paper.

References

Angrist, Joshua D, Sydnee Caldwell, and Jonathan V Hall, "Uber vs. Taxi: A Driver's Eye View," *NBER Working Paper*, 2017.

Berger, Thor, Chinchih Chen, and Carl Benedikt Frey, "Drivers of disruption? Estimating the Uber effect," *European Economic Review*, 2018, *110*, 197–210.

Besbes, Omar, Francisco Castro, and Ilan Lobel, "Surge pricing and its spatial supply response," *Management Science*, 2020.

Bimpikis, Kostas, Ozan Candogan, and Daniela Saban, "Spatial pricing in ride-sharing networks," *Operations Research*, 2019, *67* (3), 744–769.

Brancaccio, Giulia, Myrto Kalouptsidi, Theodore Papageorgiou, and Nicola Rosaia, "Search Frictions and Efficiency in Decentralized Transportation Markets," Technical Report, National Bureau of Economic Research 2020.

Buchholz, Nicholas, "Spatial Equilibrium, Search Frictions and Dynamic Efficiency in the Taxi Industry," *Working Paper*, 2020.

_, Laura Doval, Jakub Kastl, Filip Matějka, and Tobias Salz, "The Value of Time: Evidence From Auctioned Cab Rides," Technical Report, National Bureau of Economic Research 2020.

Castillo, Juan Camillo, "Who Benefits from Surge Pricing?," *Working Paper*, 2019.

Castillo, Juan Camilo, Dan Knoepfle, and Glen Weyl, "Surge pricing solves the wild goose chase," in "Proceedings of the 2017 ACM Conference on Economics and Computation" 2017, pp. 241–242.

Chen, M Keith, Judith A Chevalier, Peter E Rossi, and Emily Oehlsen, "The Value of Flexible Work: Evidence from Uber Drivers," *NBER Working Paper*, 2019.

Cohen, Peter, Robert Hahn, Jonathan Hall, Steven Levitt, and Robert Metcalfe, "Using Big Data to Estimate Consumer Surplus: The Case of Uber," *NBER Working Paper*, 2016.

Dholakia, Utpal M, "Everyone Hates Uber's Surge Pricing - Here's How to Fix It," *Harvard Business Review*, dec 2015.

Diakopoulos, Nicholas, "How Uber surge pricing really works," 2015.

Einav, Liran, Chiara Farronato, and Jonathan Levin, "Peer-to-peer markets," *Annual Review of Economics*, 2016, *8*, 615–635.

Farronato, Chiara and Andrey Fradkin, "The welfare effects of peer entry in the accommodation market: The case of airbnb," Technical Report, National Bureau of Economic Research 2018.

Fréchette, Guillaume R, Alessandro Lizzeri, and Tobias Salz, "Frictions in a Competitive, Regulated Market: Evidence from Taxis," *American Economic Review (forthcoming)*, 2019.

Gavazza, Alessandro, "An empirical equilibrium model of a decentralized asset market," *Econometrica*, 2016, *84* (5), 1755–1798.

Ghili, Soheil and Vineet Kumar, "Spatial Distribution of Supply and the Role of Market Thickness: Theory and Evidence from Ride Sharing," 2020.

Hall, Jonathan, Cory Kendrick, and Chris Nosko, "The effects of Uber's surge pricing: A case study," *The University of Chicago Booth School of Business*, 2015.

Hall, Jonathan D, Craig Palsson, and Joseph Price, "Is Uber a substitute or complement for public transit?," *Journal of Urban Economics*, 2018, *108*, 36–50.

Hendel, Igal, Aviv Nevo, and François Ortalo-Magné, "The relative performance of real estate marketing platforms: MLS versus FSBOMadison. com," *American Economic Review*, 2009, *99* (5), 1878–98.

Hopenhayn, Hugo A, "Entry, Exit, and firm Dynamics in Long Run Equilibrium," *Econometrica*, 1992, *60* (5), 1127–1150.

Joskow, Paul L and Catherine D Wolfram, "Dynamic pricing of electricity," *American Economic Review*, 2012, *102* (3), 381–85.

Lazarev, John, "The welfare effects of intertemporal price discrimination: an empirical analysis of airline pricing in US monopoly markets," *New York University*, 2013.

Lee, Min Kyung, Daniel Kusbit, Evan Metsky, and Laura Dabbish, "Working with machines: The impact of algorithmic and data-driven management on human workers," in "Proceedings of the 33rd annual ACM conference on human factors in computing systems" 2015, pp. 1603–1612.

Liu, Tracy, Zhixi Wan, and Chenyu Yang, "The efficiency of a dynamic decentralized two-sided matching market," *Available at SSRN 3339394*, 2019.

Rochet, Jean-Charles and Jean Tirole, "Platform competition in two-sided markets," *Journal of the european economic association*, 2003, *1* (4), 990–1029.

_ **and** _ , "Two-sided markets: a progress report," *The RAND journal of economics*, 2006, *37* (3), 645–667.

Rosaia, Nicola, "Competing platforms and transport equilibrium: Evidence from New York City," Technical Report, mimeo, Harvard University 2020.

Salz, Tobias, "Intermediation and competition in search markets: An empirical case study," Technical Report, National Bureau of Economic Research 2020.

Shapiro, Matthew H, "Density of Demand and the Benefit of Uber," 2018.

Tarduno, Matthew, "The congestion costs of Uber and Lyft," *Journal of Urban Economics*, 2021, *122*, 103318.

Williams, Kevin, "Dynamic airline pricing and seat availability," 2020.

Wolak, Frank A, "Do residential customers respond to hourly prices? Evidence from a dynamic pricing experiment," *American Economic Review*, 2011, *101* (3), 83–87.

Yan, Chiwei, Helin Zhu, Nikita Korolko, and Dawn Woodard, "Dynamic Pricing and Matching in Ride-Hailing Platforms," *Naval Research Logistics*, 2019.

Online Appendix (Not for Publication)

A Data Preparation

Figure A1: RideAustin Trips Over Time

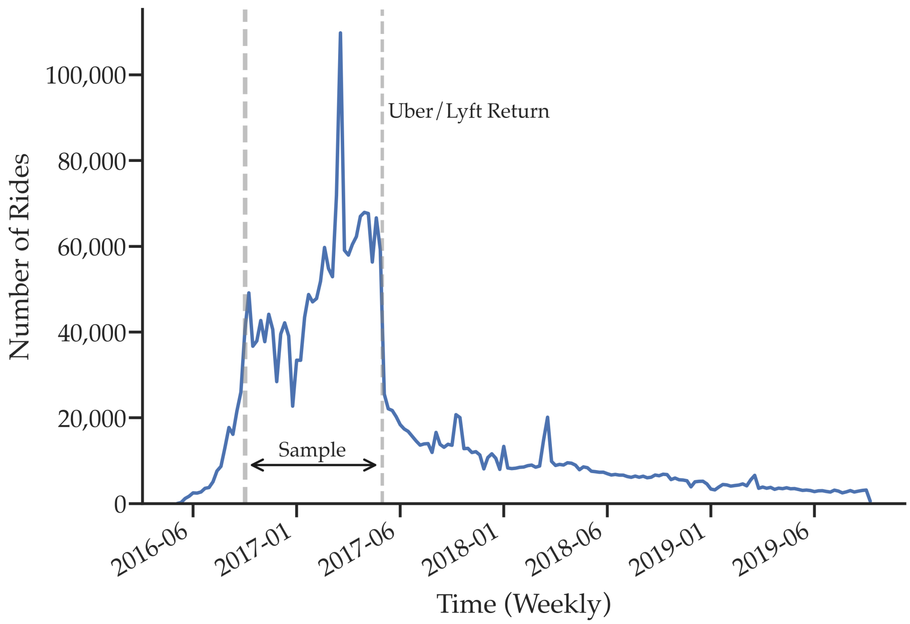

We restrict to rides between October 1, 2016 and May 31, 2017. Within this, we eliminate other rides to ensure that our data comes from a typical week. As Figure (A2) shows, within our sample period, there are two periods where this is unlikely to be true. First, is South by Southwest (SXSW), an annual festival hosted in Austin. Second, is the Christmas/New Year's holiday period. We exclude these two periods from our data. We also remove rides that are categorized as premium (a more expensive luxury option but only 5% of rides) and rides that appear to have data entry issues (3% of rides). After this, we also mostly focus on rides that begin and end inside Austin city (see Figure B3a), which further removes another 6% from the sample. In the end, we have over 1.3 million rides in the sample.

Figure A2: RideAustin Trips Over Time (October 2016–May 2017)

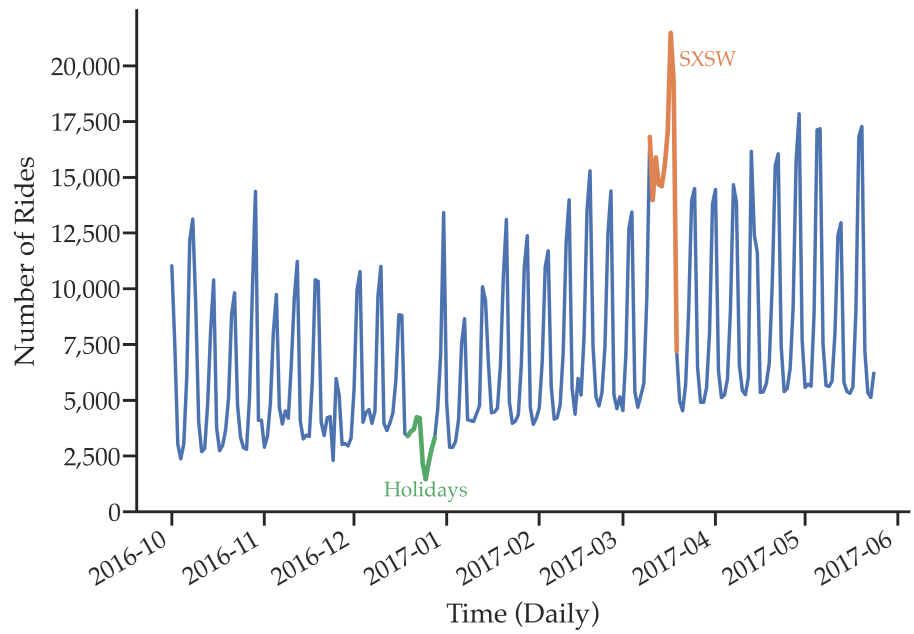

To prepare the data for the model, we focus more specifically on rides that occur on Fridays and Saturdays. The plurality of rides (46.5% of our sample) occur on these two days and they exhibit fairly similar patterns during the day.[47]

B Geographic Units

We focus on rides in Austin city. Since the official city limits are highly irregular (gray area in Figure B3), we use a collection of census tracts to approximate the boundaries of the city in a more compact manner. We then divide up this 'city region' into neighborhoods as shown in Figure (B3a). Neighborhoods are based on collections of RideAustin's surge areas (Figure B3b). These surge areas are the level at which the company sets surge. While the process of creating neighborhoods is ad hoc, we try best to mimic known neighborhoods in Austin (e.g. Downtown, South Central Austin, North Central Austin) and use reasonable boundaries (e.g. highways) as guides.

To have better notions of local demand and supply, it is useful to discretize the space into smaller units. For this we use Uber's H3 geospatial indexing system (h3geo.org) and use hexagons of resolution 8 (approximately 0.93 kilometers wide). A useful feature of this system is that it allows for a convenient way to describe the relationship (distance) between any two hexagons. In Figure (10), the red central hexagon is the reference hexagon. We can refer to the ring itself as

[47]More precisely, since our days begin at 4 a.m., we restrict to rides between 4 a.m. on Friday and 4 a.m. on Sunday.

Figure B3: Austin Map

(a) Austin Neighborhoods

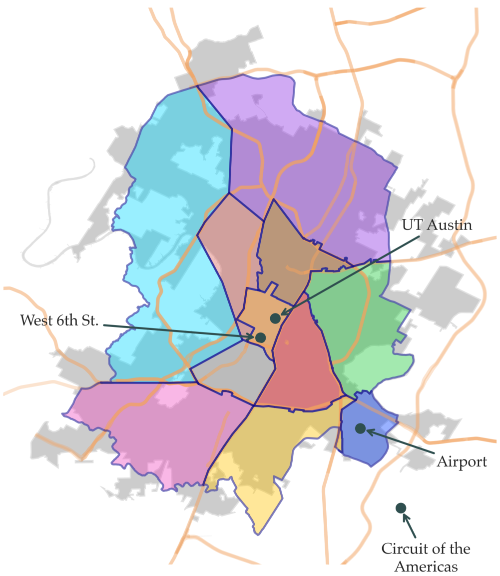

(b) RideAustin Surge Areas

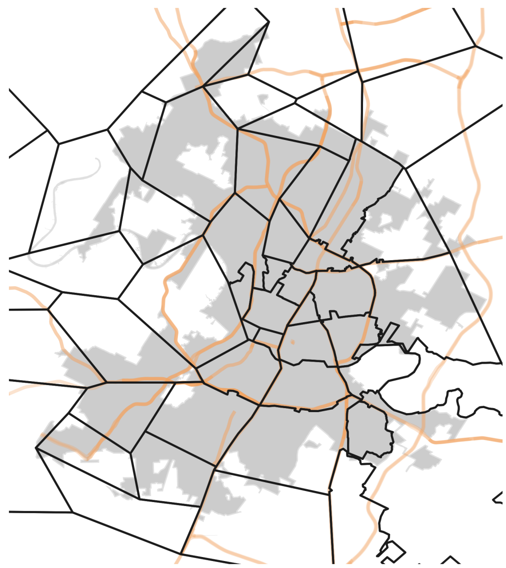

Notes: The gray area is the official municipal definition of Austin. The orange lines are highways. The colored regions are neighborhoods created by aggregating RideAustin surge areas intersected with a group of census tracts that approximate Austin city. Four points of interest are plotted on the map for illustrative purposes.

being in “ring 0”. The hexagons in blue that are adjacent to the reference hexagon are said to be in “ring 1”. This idea continues for rings 2, 3, and so on. As all hexagons are identical, we use “rings” as a measure of distance. A ring distance is equal to the hexagon’s width, i.e. 1 ring is approximately 1 kilometer.

Given that suburban areas are not dense and feature a very small fraction of our rides, we aggregate hexagons in the suburbs to reduce the dimensionality of our state space. This greatly reduces the computational burden in the model estimation. To do this, we find the weighted centroid of ride locations (start and end coordinates) within each surge area. We then map this centroid to a hexagon and take that to be the representative hexagon of the surge area. For the areas in the central part of the city, we do not do this aggregation as these are high activity areas in our data. In the end, we are left with 83 locations in the city as shown in Figure (B4). 54 of these are in the central part and are not aggregated; these are plotted in yellow in the figure. 86% of rides start or end in these hexagons, so this level of aggregation does not create too much data loss. This aggregation has an implication for distances in the model. We can partition the city into the central areas ($\mathcal{J}_C$) and non-central areas ($\mathcal{J}_N$), i.e. $\mathcal{J} = \mathcal{J}_C \cup \mathcal{J}_N$. To calculate distances, we set $\delta_{ij} = Ring(i, j)$ if $i \neq j$ or $i = j \in \mathcal{J}_C$. For $i = j \in \mathcal{J}_N$, we set δ_{ii} as the average ring distance between all the hexagons that i is a representative for.

In the model, we restrict which hexagons can be accessed from each hexagon via the correspondence $A(i)$. This is graphically represented in Figure (B4). This can be thought of as capturing main streets and highways. We create these routes by assigning each hexagon access to all routes within ring 2 (areas it can access within one time period). For hexagons that have fewer than 6 connections from this (i.e. the areas in the periphery), we assign them access to the three nearest outer hexagons (in blue) and the three nearest central hexagons (in gold). All access routes are symmetrical (i.e. if area i can access j, then j can also access i).

Finally, our estimation relies on moments capturing average entry and exit. We divide up our neighborhoods into three regions, as shown in Figure (B5). The region numbers capture the centrality of the area, where Region 1 is the central downtown neighborhood.

C Additional Summary Statistics

In Figure (C6), we plot the distribution of the average number of rides per day for a driver. We calculate this in two ways. The first method (driver-day count) treats each driver in each day as a separate unit of observation. Here, we see that distribution is heavily right-skewed, with a mode of only 1 ride. The second method (within-driver average) plots the average number of trips that a driver makes within a day across all the days that we observe said driver having a ride. In contrast to the first approach, this distribution is less skewed. This difference has an important

Figure B4: Model Map

(a) Representative Hexagons

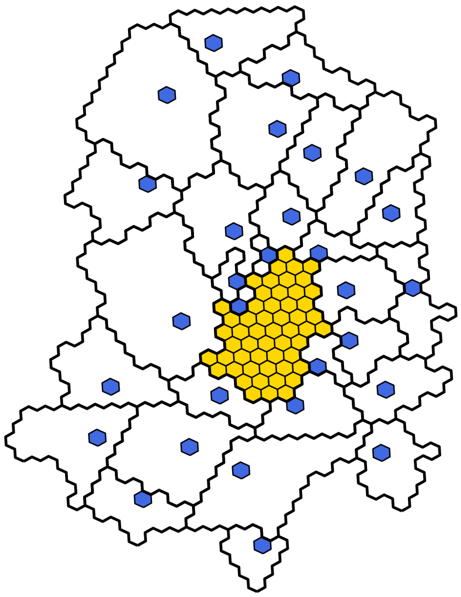

(b) Access Routes

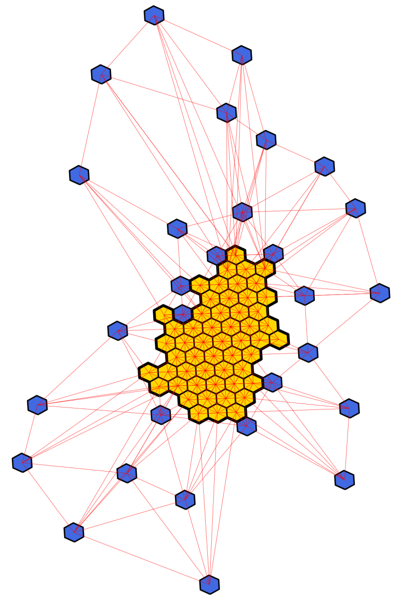

Notes: This represents the map used in the model, where each hexagon is a location. The yellow central hexagons are unaggregated. The blue outer hexagons are representative of a broader area. In (a), the black borders capture the area which the representative hexagon covers. In (b), a line connecting two hexagons represents a route (i.e. connection) between the two hexagons.

– and intuitive – interpretation. On average, a driver may expect to have 3-6 rides per day; this translates to working for about an hour. However, on an individual day, a driver's actual rides could vary widely from days with only one ride to days with over 15 rides. This is what one would expect given that ridesharing is part of the 'gig economy' where drivers supplement their income by driving for short shifts in the day, but that this income source is quite volatile. This also implies that entry and exit decisions of drivers are crucial in any model of the ridesharing market, in sharp contrast to the traditional taxi market as modeled by Buchholz (2020).

Figure B5: Regions

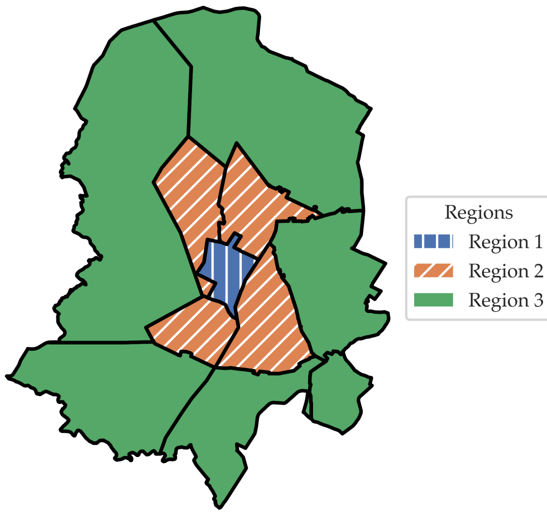

Figure C6: Distribution of Rides per Day

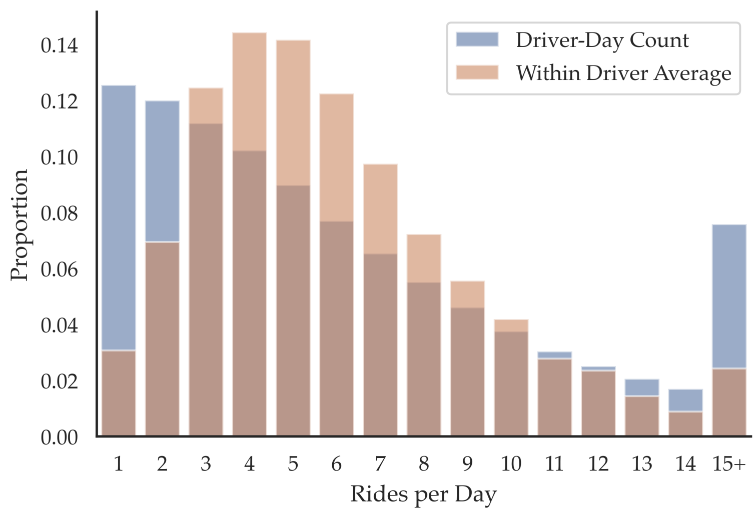

Notes: Let N_{it} be the number of rides taken by driver i on day t. Driver-day plots the non-zero distribution of $\{N_{it}\}_{i,t}$. Within-driver average plots the distribution of $\left\{\frac{1}{\sum_t \mathbb{1}\{N_{it}>0\}} \sum_t N_{it}\right\}_i$.

Table C8: Probability of Exit

Start Region	**End Region** *Region 1*	*Region 2*	*Region 3*
Region 1	14.2	16.5	24.3
Region 2	14.1	15.9	22.8
Region 3	13.2	14.9	19.5
	$N = 1,053,069$		

Notes: Each cell represents the proportion of trips that that start in Region i (row) and end in Region j (column) that are driver's last ride. Last ride is defined as a ride where the driver has no subsequent trips for the next 60 minutes. See Figure (B5) for regions.

Figure C7: Distribution of Trips (by End Location)

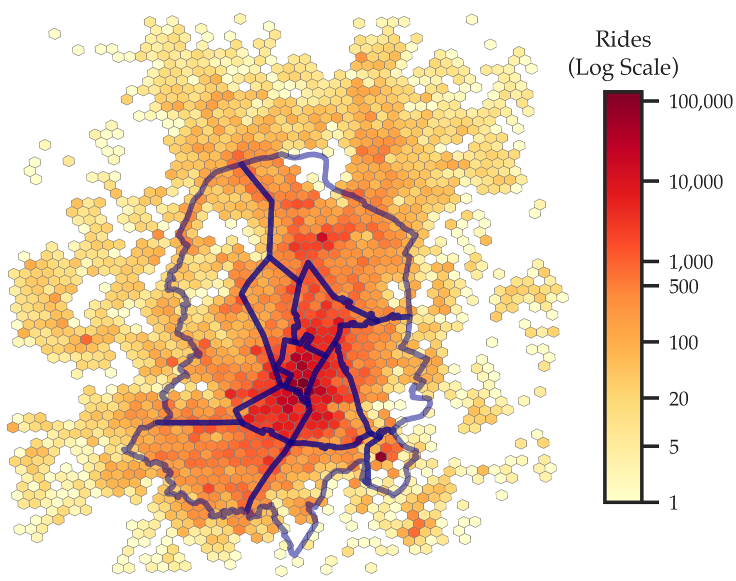

Figure C8: Wait Time By Pick-Up Location

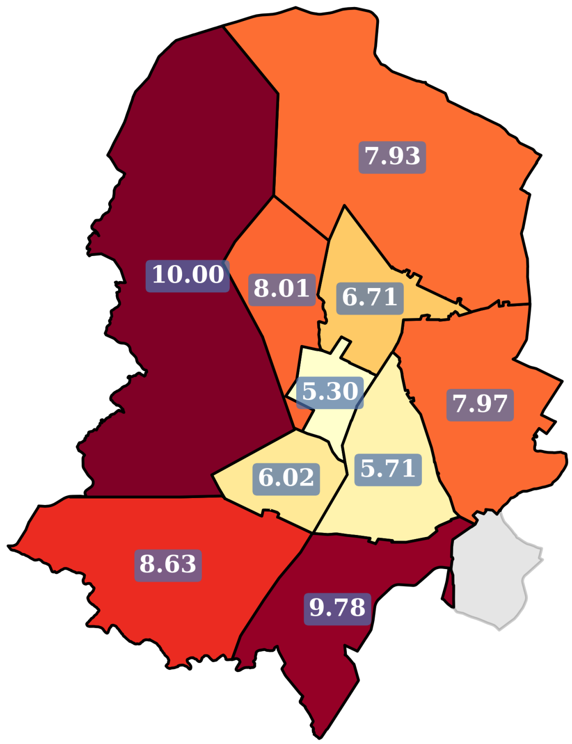

Notes: This plot shows the mean waiting time by neighborhood for riders requesting trips.

Figure C9: Exit Rates by Neighborhood

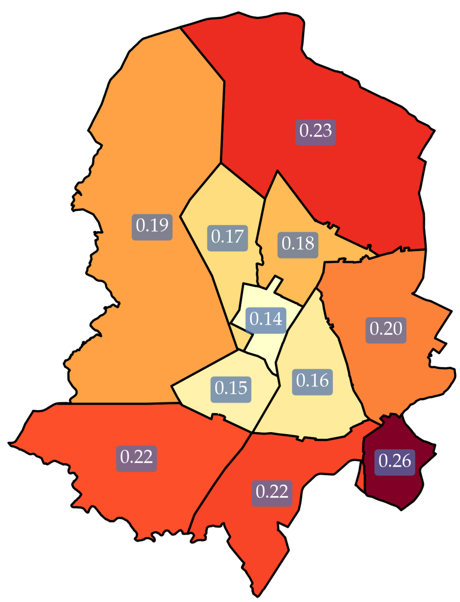

Notes: For each neighborhood, the value represents the proportion of trips that end in the neighborhood which are a driver's last ride. Last ride is defined as a ride where the driver has no subsequent trips for the next 60 minutes.

Figure C10: Active Drivers Within Day

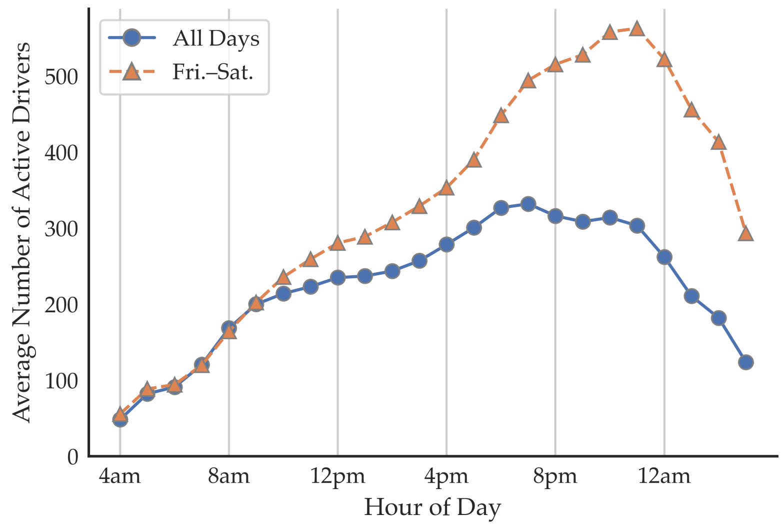

Notes: This plots the average number of active drivers (searching or in a trip) by hour of the day for the full sample (All Days) and the model sample (Fri.–Sat.).

Figure C11: Rider Wait Time Distribution

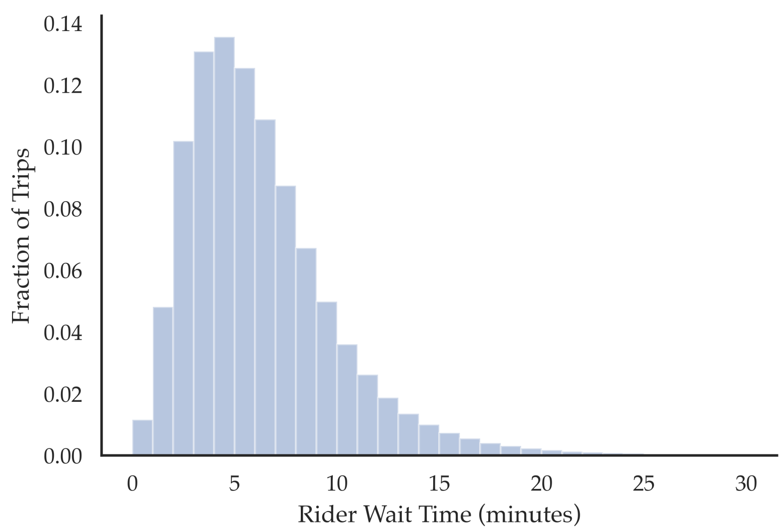

Figure C12: Time Searching Between Rides

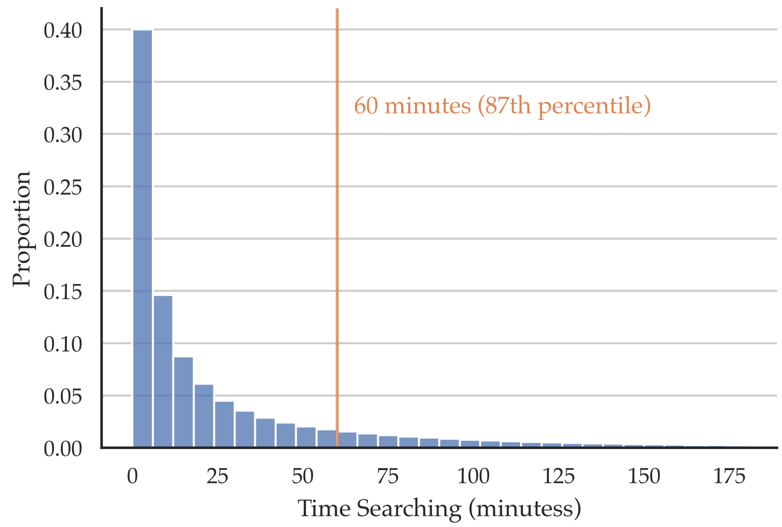

Figure C13: Shift Length by Starting Hour

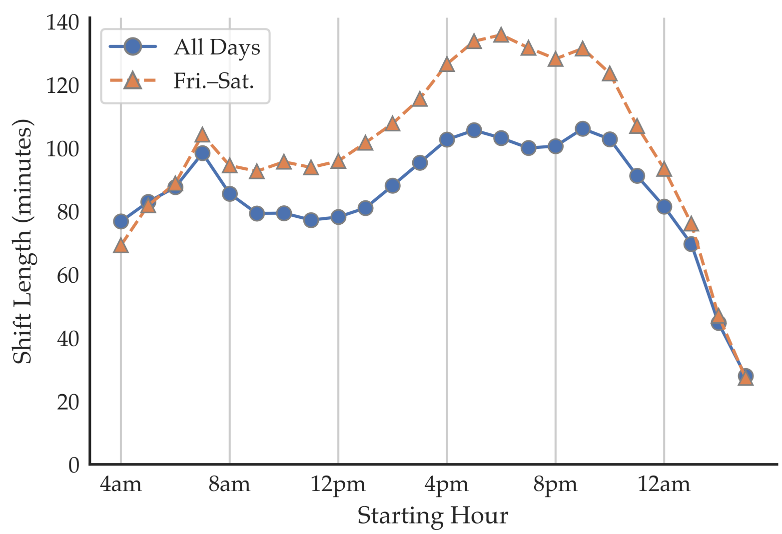

Notes: This plots the average shift length by the hour in which the shift starts. This is done for both the full sample (All Days) and the model sample (Fri.–Sat.). A shift begins when a driver is dispatched for the first time after 60 minutes of having no trips in a given day. A shift ends when the driver completes a trip with no subsequent trips in the next 60 minutes within that same day.

Figure C14: Surge versus Demand/Supply Ratio

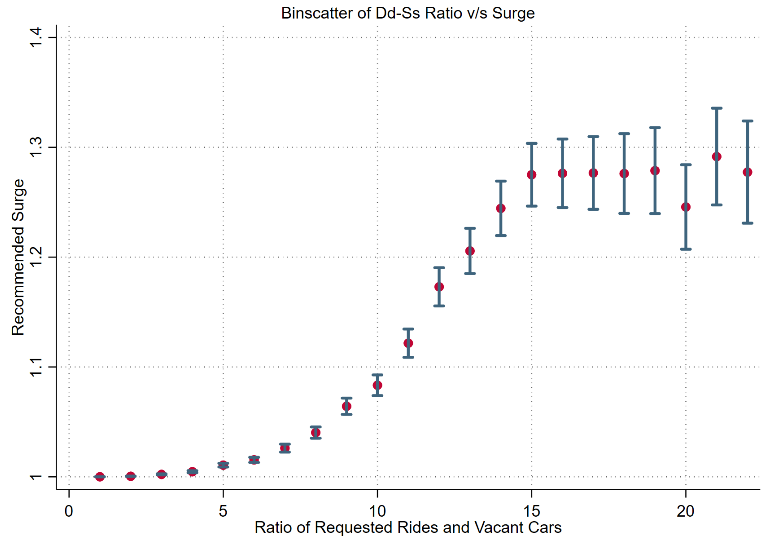

Figure C15: Recommended versus Actual Surge

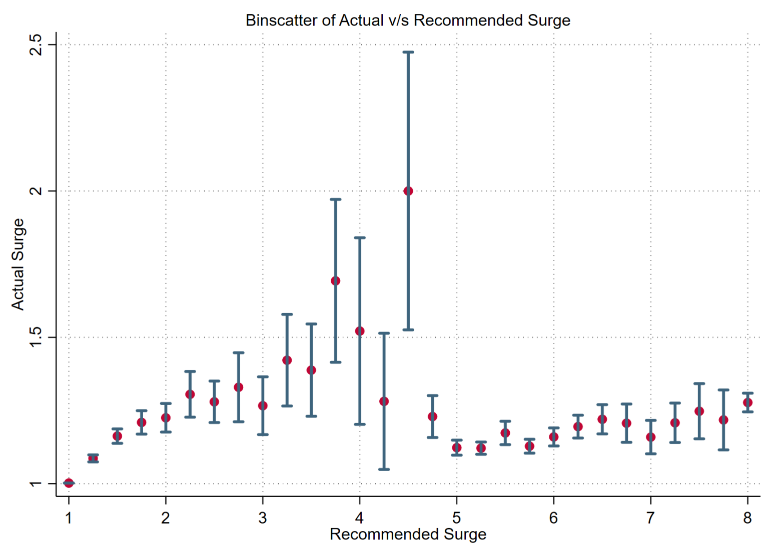

Figure C16: Distribution of Pull Distances

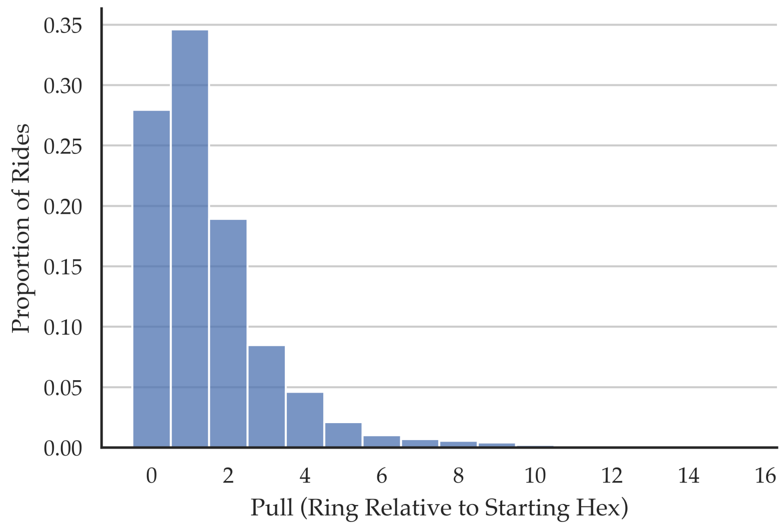

D Model Details

D.1 Matching Algorithm

The first three stages of the matching procedure is illustrated in Figure (D17) for two hexagons highlighted in yellow. First, all demand within the yellow hexagons are met using a Leontief matching function. If there is still unmet demand in those hexagons, then we match drivers in Ring 1 to the remaining riders in the yellow hexes. This can be seen in panel (b) of Figure (D17) as pulling from the blue hexagons. If there is still unmet demand in the yellow hexagons, we move on to Ring 2 as denoted in panel (c) of Figure (D17) and match available drivers to remaining riders.[48]

[48]For illustrative purposes, this figure only shows the matching for two hexagons. The full algorithm is done simultaneously for all hexagons in every time period t.

Figure D17: Matching Procedure

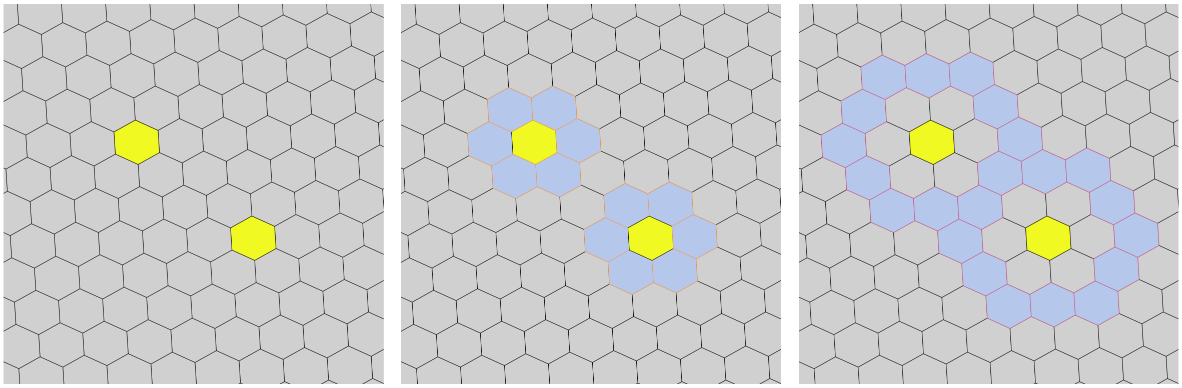

Figure 3 (a) **Figure 3 (b)** **Figure 3 (c)**

We want to show that our matching algorithm is empirically justified, in particular, that RideAustin aims to match riders to the nearest available driver. Figure (D18) shows that as the time between successive rides in the same location is small, then riders are matched to drivers who are on average further away. The reasoning behind this pattern is simple. Consider two riders who request rides from the same location within minutes of each other. Then, once the first rider has been matched to a driver, the supply of drivers is temporarily reduced in that location and its neighboring areas. So one would expect that the second rider is matched to a driver who is further away than the first driver if RideAustin matches riders to the closest riders. This is precisely the pattern we see in Figure (D18), where we plot the difference in time between successive rides on the x-axis against the difference in distance to the riders for the two drivers. As the time between successive ride requests gets smaller, then the difference in distance to the riders gets larger. On the other hand, as the time between successive rides increases, the market gets more time to adjust and thus the drivers are approximately the same distance away from the riders.

Figure D18: First Dispatch Protocol Observed in the Data

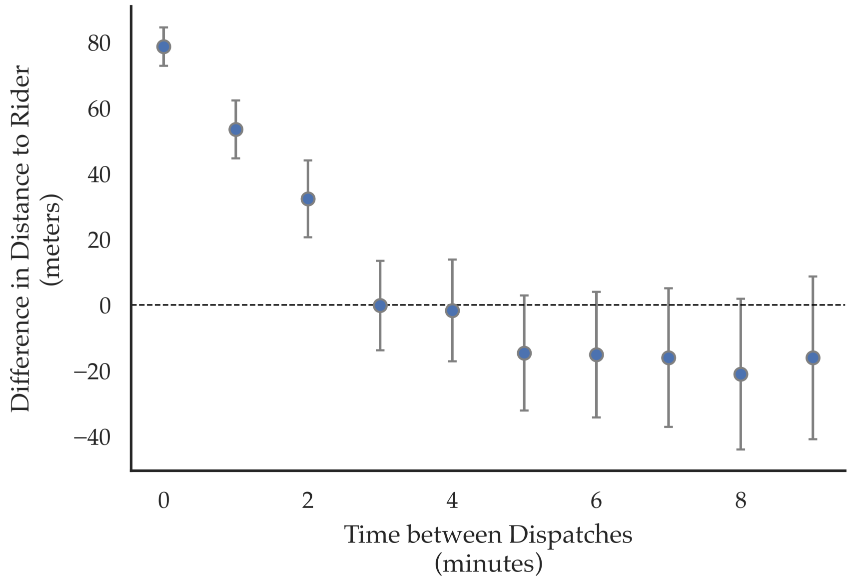

Notes: The x-axis captures the difference in dispatch time for two successive rides in the same location. The y-axis is the average difference in distance the drivers are from their rider. The x-axis values are binned at 1 minute intervals.

D.2 Surge Pricing Algorithm

We use the elements of the data to motivate a two-step approach. In the data, we observe for every area a and 5-minute interval t, the number of people requesting trips (demand), the number of vacant drivers (supply), a recommended surge factor, and an actual surge factor.[49] In the first step, the algorithm computes a deterministic recommended surge factor $\tilde{s}_a^t$ for every area a and 5-minute interval t based on local market conditions. In the second step, it converts the recommended surge $\tilde{s}_a^t$ into the actual surge factor s_a^t (the value that agents observe) using a probabilistic approach.[50] We estimate both of these steps based on the empirical patterns seen in the data.

To determine the recommended surge, we fit a function to predict the recommended surge based on demand and supply across locations and time periods. In Figure (C14), we see that there is a strong relationship between surge and the ratio of the demand and supply of rides, thus providing support for this approach. We estimate the following equation:

$$\tilde{s}_{ad}^t = \gamma_1 \text{Demand}_{ad}^t + \gamma_2 \text{Supply}_{ad}^t + \gamma_3 s_{ad}^{t-1} \times \mathbb{1}\left\{\tilde{s}_{ad}^{t-1} > 1\right\} + \alpha_a + \lambda^t + \varepsilon_{ad}^t \qquad (11)$$

[49] This data is not observable in our trips dataset. However, as mentioned in 2.2, we have access to a separate dataset which has this information.

[50] As shown in Table (1), the actual surge factor s_a^t goes up in increments of 0.25 starting at 1. The surge factor never goes below 1.

In the above equation, a indicates a surge area (rather than a hexagon), t is a 5-minute interval, and d is a day in our sample. $\mathbb{1}\{\tilde{s}_{ad,t-1} > 1\}$ is an indicator which turns on if the recommended surge in the previous period was bigger than 1. This captures the persistence of surge in a location once it is activated. We use the estimated parameters from Equation (11), to calculate the recommended surge $\tilde{s}_a^t$ in the first step of our algorithm.

For the second step, we convert the recommended surge into actual surge using a probabilistic approach.[51] Each recommended surge factor is converted to an actual surge factor with some probability. We determine these probabilities using the empirical distribution in the data. Denote F as the set of actual surge factors which we observe in our data. Given a fixed recommended surge $\tilde{s}$, we can compute from our data the probability of actual surge being $s \in F$. The model converts $\tilde{s}_a^t$ to s_a^t using draws according to the estimated probabilities.

D.3 State Transition

Here, we specify the state transition process as a function of the key variables. We consider the transition from $\mathcal{S}^t = \{v_i^t, r_i^t\}_{i\in\mathcal{J}}$ to $\mathcal{S}^{t+1} = \left\{v_i^{t+1}, r_i^{t+1}\right\}_{i\in\mathcal{J}}$.

The total number of drivers available at location i at time $t+1$ depends on:

(i) the number of drivers who reach location i at time $t+1$ after choosing to search there

(ii) the number of drivers who drop off passengers there

(iii) the number of drivers who choose to enter in that location

Vacant drivers choose to search or exit according to the policy function σ_i^t (Equation 7) and potential drivers choose to enter with the policy functions q_i^t (Equation 9). Drivers drop off passengers according to the probabilities denoted by M_{ij}^t (Equation 4). Call the history of spatial distribution, destination probabilities, and surge as $H^t = \{\mathcal{S}^z, M^z, s^z\}_{z=1}^t$. The state transition kernel of driver location is therefore defined as:

$$Q\left(v^{t+1}\,\middle|H^t\right) = \sum_{z=1}^{t}\left(\underbrace{Q_S\left(v_S^{t+1}\,|\mathcal{S}^z, \sigma^z\right)}_{\text{Drivers arriving from search}} + \underbrace{Q_T\left(v_{IT}^{t+1}\,|H^z\right)}_{\text{Drivers completing trips}}\right) + \underbrace{Q_E\left(\bar{v}^{t+1}\,\middle|\mathcal{S}^t, q^t\right)}_{\text{New drivers entering}} \tag{12}$$

where v is the vector of total vacant drivers, v_S is the vector of searching drivers, v_{IT} is the vector of in-transit drivers who are engaged in trip, and $\bar{v}$ is the vector of entering drivers. The transition kernel for searching drivers, matched drivers finishing trips, and entering drivers are denoted by Q_S, Q_T, and Q_E, respectively. Note that the transitions rely on the history of states

[51] Figure (C15) in the Appendix shows that on average the actual surge is lower than the recommended surge, though there can be large variation.

and policy functions, rather than just those from t, as drivers can take multiple periods to arrive from their search or assigned trip (however, new drivers simply enter based on the current period's conditions).

The transition kernel for demand is $Q_R\left(r^{t+1}\,|H^t, \varpi\right)$, where next period's demand is a function of the current period's surge and the exogenous drop-out probability ϖ. Together, the transition kernel of driver location Q and the transition kernel of demand Q_R determine the state transition of $\mathcal{S}^t$ to $\mathcal{S}^{t+1}$.

D.4 Equilibrium

The equilibrium in our setting is determined by the driver's beliefs about the entire distribution of riders and drivers across space as well as the beliefs over the preferences of consumers to be dropped off in different locations. Denote this belief of a driver in location i as $\tilde{Q}_i^t$. Given that the drivers' optimal policies only depend on the current state and their beliefs about the evolution of the state, we can define the following Markovian equilibrium in our setting similar to Buchholz (2020).

Definition. Equilibrium is a sequence of state vectors $\{\mathcal{S}^t\}$, transition beliefs $\left\{\tilde{Q}_i^t\right\}$, and policy functions $\{\sigma_i^t, q_i^t\}$ over each location $i \in \mathcal{J}$ and an initial state $\{\mathcal{S}_i^0\}$ such that:

1. In each location $i \in \{1, 2, \ldots, L\}$, at the end of each period, unmatched drivers search or exit according to their policy functions $\{\sigma_i^t\}$, which solves Equation (5), and derive expectations under beliefs $\tilde{Q}_i^t$. This determines the transition kernel of unmatched drivers given by $Q_S\left(v_S^{t+1}\,|\mathcal{S}^z, \sigma^z\right), \forall z \in [0, 1, ..., t]$.

2. In each location $i \in \{1, 2, \ldots, L\}$, at the start of each period, potential drivers enter according to their policy functions $\{q_i^t\}$, which solves Equation (8). This determines the transition kernel of entering drivers given by $Q_E\left(\bar{v}^{t+1}\,|\mathcal{S}^t, q^t\right)$.

3. In each location $i \in \{1, 2, \ldots, L\}$, at the start of each period, in transit drivers arrive at drop-off locations following the transition matrix M^t. This determines the transition kernel for matched drivers $Q_T\left(v_{IT}^{t+1}\,|H^t\right), \forall z \in [0, 1, ..., t]$.

4. The state transitions are given by the combination of matched, unmatched, and entering drivers which is given by Equation (12).

5. Driver's expectations are rational which implies that the transition beliefs are self-fulfilling given the optimizing behavior i.e. $\tilde{Q}_i^t = Q_i^t$ for all i and t.

Algorithm 1 Algorithm Describing the Equilibrium Computing Algorithm

Input the demand and empirical consumer match probabilities M^t
Fix parameter σ_ε and guess initial $\mathcal{S}_0^T$ and compute $V^T(\mathcal{S}_0^T)$
while diff ¿ tol **do**
  Set counter $k = 0$
  for $t = T - 1$ to 1 **do**
    Guess $\mathcal{S}_0^t$ and compute $V^t(\mathcal{S}_0^t)$
    Derive choice specific value functions $W_i^t(j, S^t)$ for all i, j, t
    for $t = 1$ to $T - 1$ **do**
      Derive policy functions σ from choice specific value
      σ, M, and q imply transition from $\mathcal{S}^t$ to $\mathcal{S}^{t+1}$
      Update $\mathcal{S}_k^t$ and V_k^t to $\mathcal{S}_{k+1}^t$ and V_{k+1}^t
      $k = k + 1$
    end for
  end for
  Compute diff = max—$V_{k+1} - V_k$—
end while

Figure D19: 12 am. to 3 a.m. Value Functions

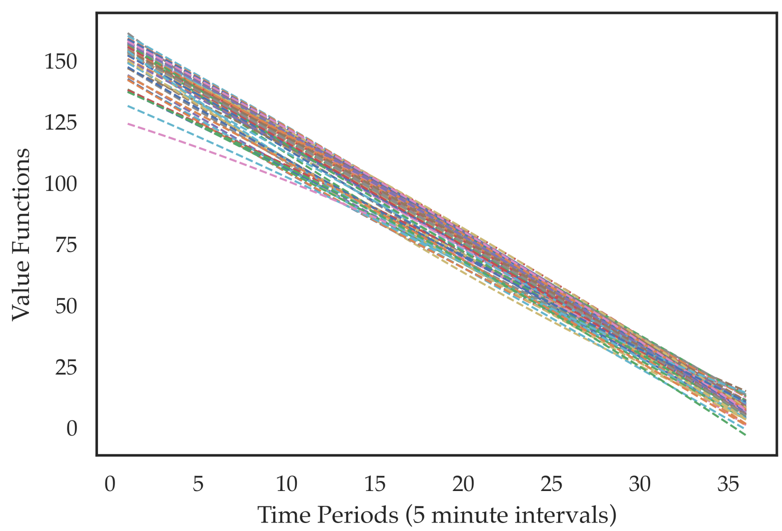

Figure D20: 12 am. to 3 a.m. Convergence

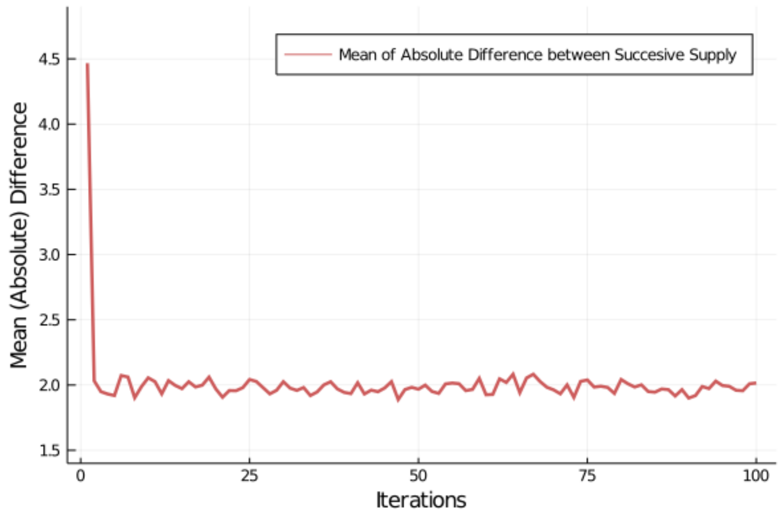

Notes: This graph plots the mean absolute difference between successive supply matrices over 100 iterations of the equilibrium algorithm that we use. On average there is a change of 2 drivers in a single location across successive iterations. Given that most suburban areas rarely have any drivers and that drivers are concentrated in central Austin, this implies that a change of less than 2 drivers is unlikely to change equilibrium driver behavior.

E Demand Elasticities

Table (E9) shows how the price and waiting time elasticity vary through the day. The first two columns present results from 3 p.m. to 9 p.m. while the last two columns present results from 9 p.m. to 3 a.m. The price elasticity of demand is much higher during the day/evening than late at night while the waiting time elasticity is higher at night.

Table E9: IV Demand Results

	1st Stage (3 pm - 9 pm)	2nd Stage (3 pm - 9 pm)	1st Stage (9 pm - 3 am)	2nd Stage (9 pm - 3 pm)
	Surge (Log)	(Log) Rides Requested	Surge (Log)	(Log) Rides Requested
Surge (Log)		-2.16**		-0.18
		(0.98)		(0.20)
# Completed Rides (Log)	-0.0050***		-0.022***	
	(0.00)		(0.00)	
Wait time (Log)	0.0094***	-0.015	0.018***	-0.034***
	(0.00)	(0.01)	(0.00)	(0.01)
# People Opening App (Log)	0.011***	0.022**	0.017***	0.0027
	(0.00)	(0.01)	(0.00)	(0.00)
Area× Time Interval FE	Yes	Yes	Yes	Yes
F - stat	22.90	.	270.04	.
Observations	28139	28139	21896	21896

This table presents the results from using both number of rides ending in location i at time t as well as the lagged number of ending rides to instrument for price and waiting time.

Table E10: IV Demand Results with Two IVs

	First Stage		Second Stage
	Surge (Log)	Wait time (Log)	(Log) Rides Requested
# Completed Rides (Log)	-0.0084***	0.098***	
	(0.00)	(0.00)	
Lagged Completed Rides (Log)	-0.0032***	-0.064***	
	(0.00)	(0.00)	
# People Opening App (Log)	0.010***	-0.0078***	0.021***
	(0.00)	(0.00)	(0.00)
Surge (Log)			-2.44***
			(0.38)
Wait time (Log)			-0.23***
			(0.06)
Area× Time Interval FE	Yes	Yes	Yes
F - stat	309.14	259.76	.
Observations	134368	134503	80387

F Model Fit and Counterfactuals

F.1 Model Fit

Table F11: 3 p.m. to 6 p.m. Shift - Non-targeted Moments

	Data	**Benchmark**	**No Surge**	**No Match**	**Gig Taxi**
Average Earnings	31.51	27.63	25.76	21.67	19.16
Surged Rides (%)	18.96	17.08	0.00	18.15	0.00
Unmet Demand (%)	–	4.44	5.77	29.29	30.79
Last Rides (%)	40.16	46.59	45.17	55.46	56.19
Average Search Distance	–	16.61	16.42	19.08	20.07
Number of Trips	1,197	1,247	1,242	898	897
P(Search in Region 1)	–	0.39	0.40	0.37	0.36
P(Search in Region 2)	–	0.57	0.56	0.59	0.60
P(Search in Region 3)	–	0.04	0.04	0.04	0.04

Notes: Average Earnings is the average revenue earned by a driver. Surged Rides is the proportion rides which are surged. Unmet Demand is the proportion of requested rides which were unmet. Last Rides is the proportion of total rides which were last rides for a driver. Average Search Distance is the ring distance between the dropoff location for trip k and dispatch location of trip $k + 1$. P(Search in Region i) refers to the proportion of total searches in Region i

Table F12: Non Targeted Moments

	Afternoon		*Evening*		*Night*		*Late Night*	
	Data	**Model**	**Data**	**Model**	**Data**	**Model**	**Data**	**Model**
Average Earnings	31.51	27.63	34.97	25.50	42.62	26.52	54.56	39.83
Surged Rides (%)	18.96	17.08	21.44	19.80	22.23	20.45	46.88	48.10
Last Rides (%)	40.16	46.59	32.67	47.70	27.64	46.52	26.38	36.64
Number of Trips	1,197	1,247	1,977	1,434	2,494	1,550	2075	1632

Notes: Average Earnings is the average revenue earned by a driver. Surged Rides is the proportion rides which are surged. Last Rides is the proportion of total rides which were last rides for a driver.

Figure F21: Distribution of Surge in the Data and Model

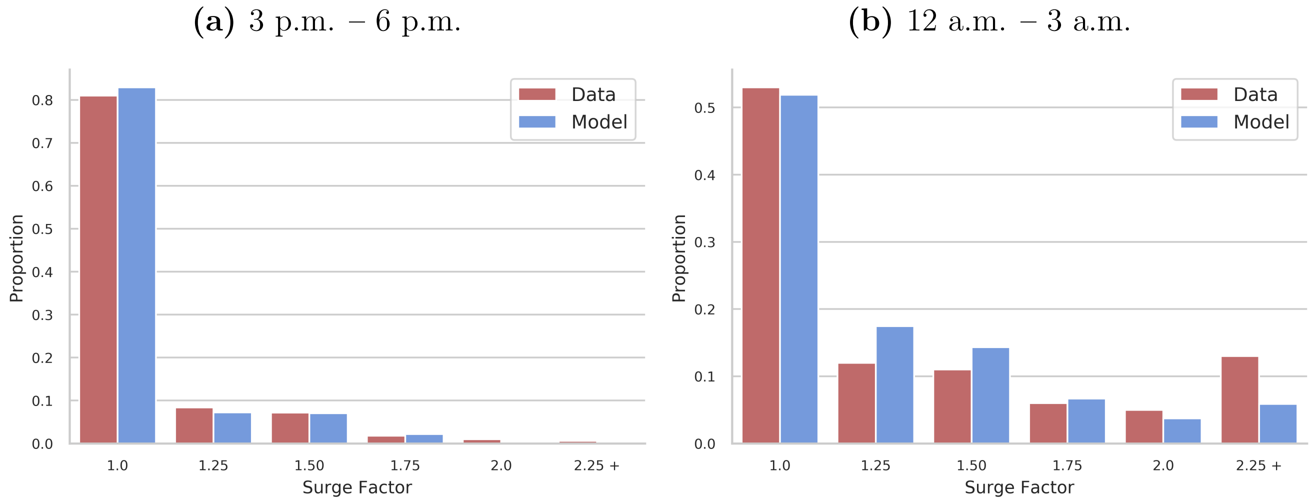

Notes: In panel (a), we show how the distribution of surge factors from the model compares to the distribution from the data. In panel (b), we show this for the late night shift. The results for the other two shifts are similar.

Figure F22: Spatial Distribution of Proportion of Unmet Demand (3 p.m. – 6 p.m.)

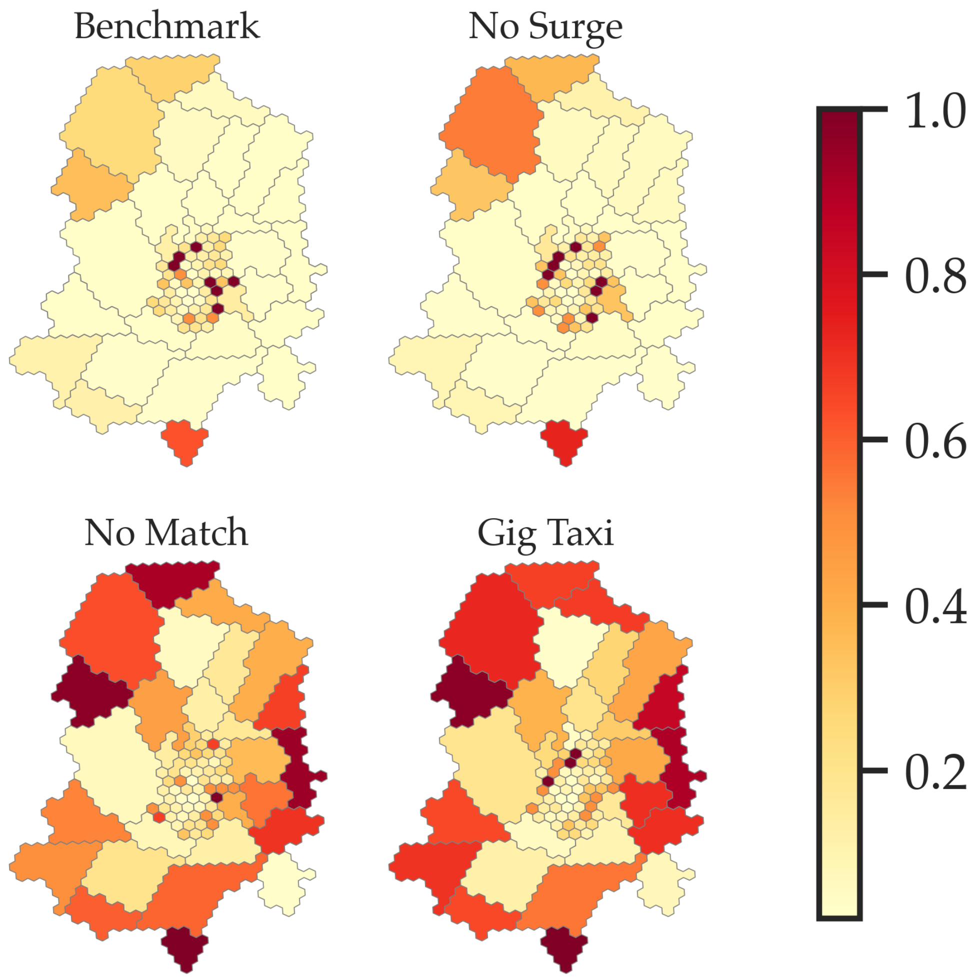

Notes: This figure shows the spatial distribution of the proportion of rides which are requested go unmatched.

F.2 Additional Counterfactual Results

Figure F23: Average Pull versus End-Start Difference

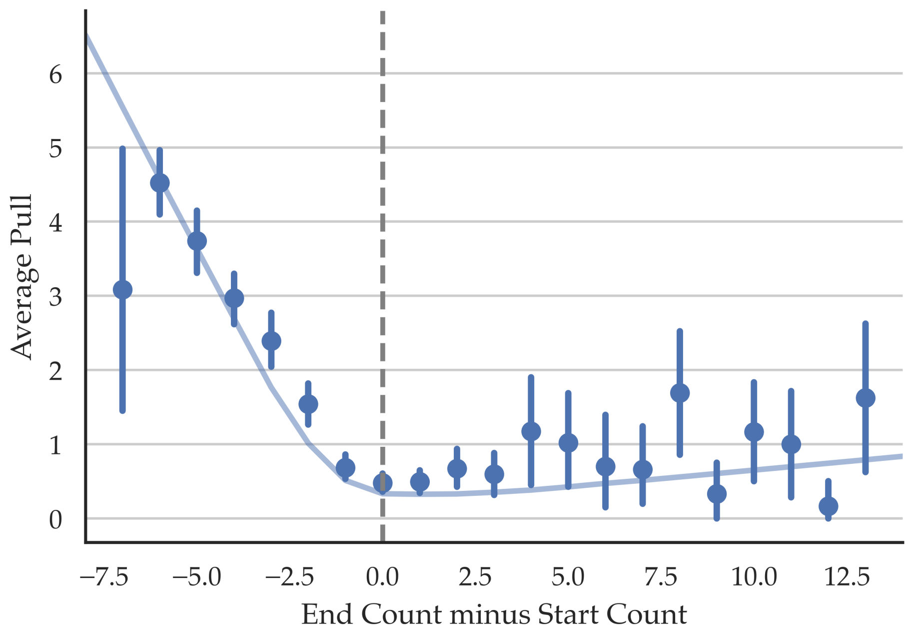

Notes: This is a binned scatter plot, where each unit of observation is a location-time cell as shown in Figure (**??**). The x-axis represents the difference in the count of rides ending in the location-time and the count of rides starting in the location-time. We restrict to x-axis values between the 1st and 99th percentile of the distribution. The y-axis represents the average pull for rides in the corresponding bin. The line represents a LOWESS function line. The results are shown from the benchmark model.

Figure F24: Spatial Distribution of Consumer Surplus (12 a.m. – 3 a.m.)

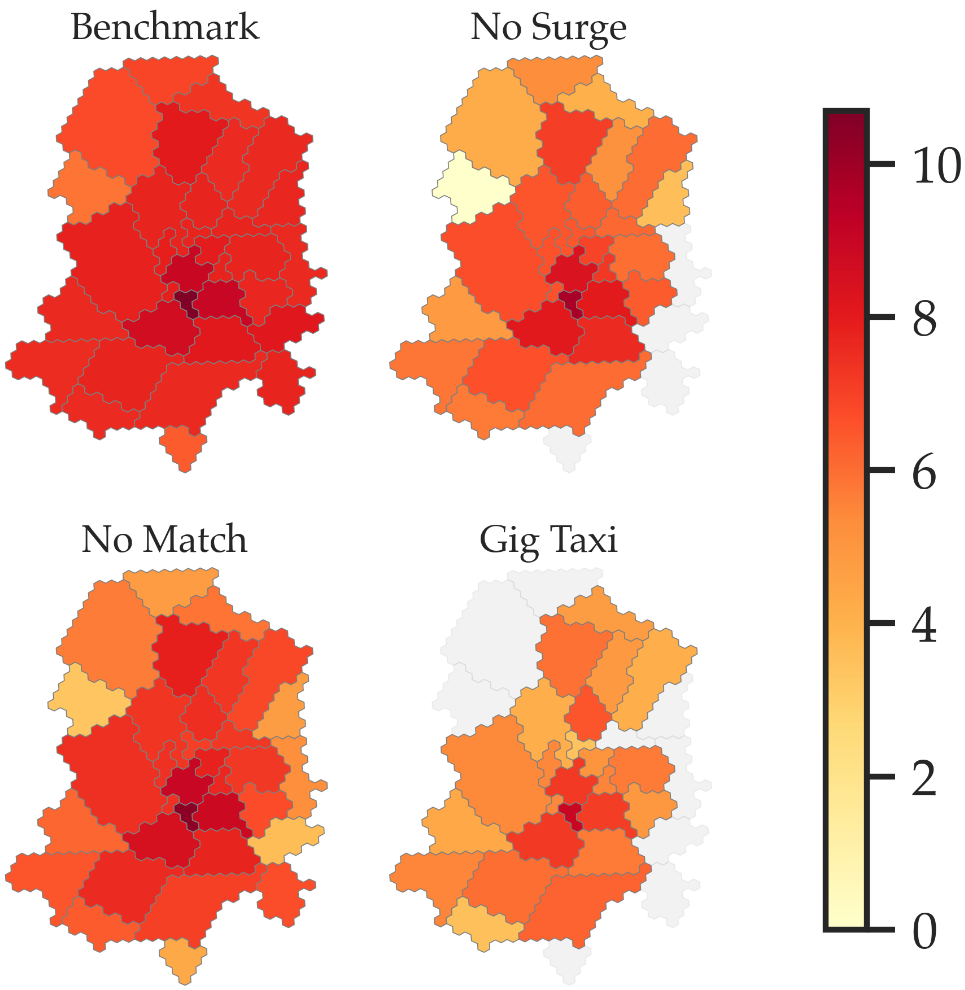

F.3 Complementarities

To expand on the complementarity, while surge pricing induces more drivers to enter, it can only indirectly allocate drivers to where they are needed. Matching not only corrects the spatial misallocation issue, but allows the platform to rely less on surge. With a lower surge, more consumers will request rides, and the matching technology almost certainly ensures they will be picked up. However, matching pulls drivers farther, especially if there are not enough drivers to satisfy all of demand. When surge pricing is added – and more drivers enter – this will lead to lower pull distances than without it.

The complementarities between surge and matching also interact with the third feature of ridesharing: that drivers can choose to enter and exit throughout the day. Indeed, surge pricing is effective in large part because it induces drivers to enter the market. However, under a taxi system where supply is fixed (i.e. drivers cannot enter and exit), there is smaller scope for surge pricing to increase welfare. This is seen in Figure (F25) and (F27) by comparing the surged taxi counterfactual to the dotted line. This counterfactual performs worse than the taxi equilibrium irrespective of the time of day. Matching is also highly effective because it can re-allocate drivers without the risk of incentivizing drivers to exit due to pulling them to locations they do not want to be.

Figure F25: Welfare Comparison (12 a.m. – 3 a.m.)

Surge	True	False	True	True	True	False	False
Matching	True	True	False	True	False	True	False
Entry/Exit	True	True	True	False	False	False	True

To make the point in Section 7.4.1 clearer we consider another driver compensation scheme where drivers keep a proportion α of the trip revenue instead of paying a \$0.99 fee so as to keep their total earnings the same. This α is calculated to be 92% of the trip revenue. We re-run our model with drivers keeping 92% of the trip revenue instead of paying a \$0.99 fee and find no difference from the benchmark results. This is seen in Figure (F26). This is driven by the fact that the lump-sum fee affects the extensive margin (entry and exit), which is highly responsive to prices, while the proportional compensation scheme affects the intensive margin as well (search), which is not as responsive to prices.

Figure F26: Comparison of Driver Compensation Scheme with $\alpha = 0.92$

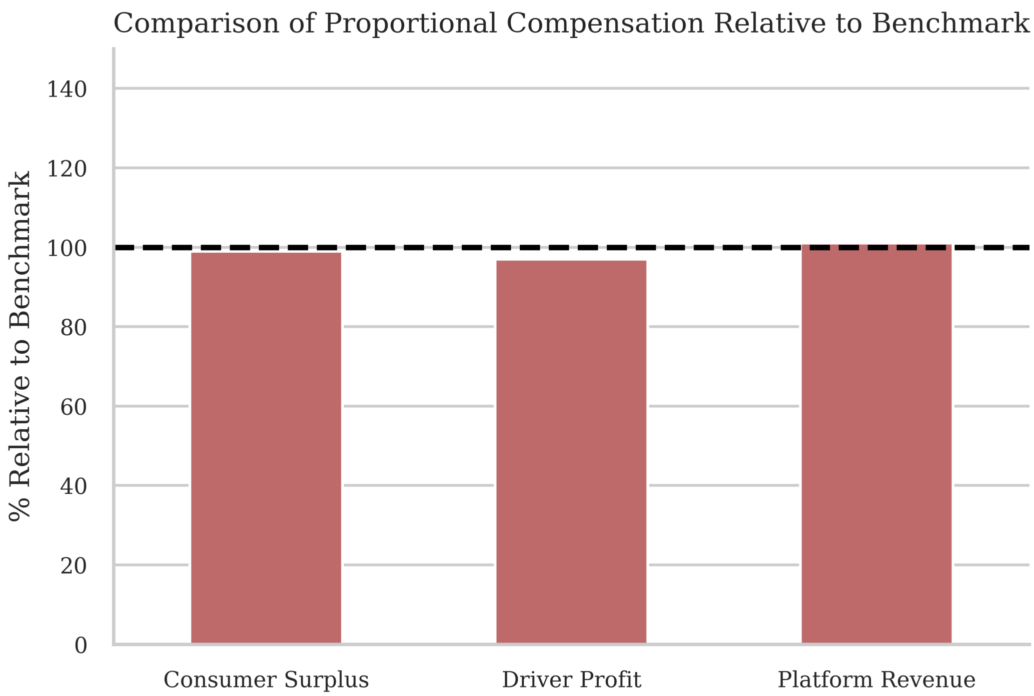

Figure F27: Welfare Comparison (3 p.m. – 6 p.m.)

Surge	True	False	True	True	True	False	False
Matching	True	True	False	True	False	True	False
Entry/Exit	True	True	True	False	False	False	True

Figure F28: Effects of Varying Matching and Surge

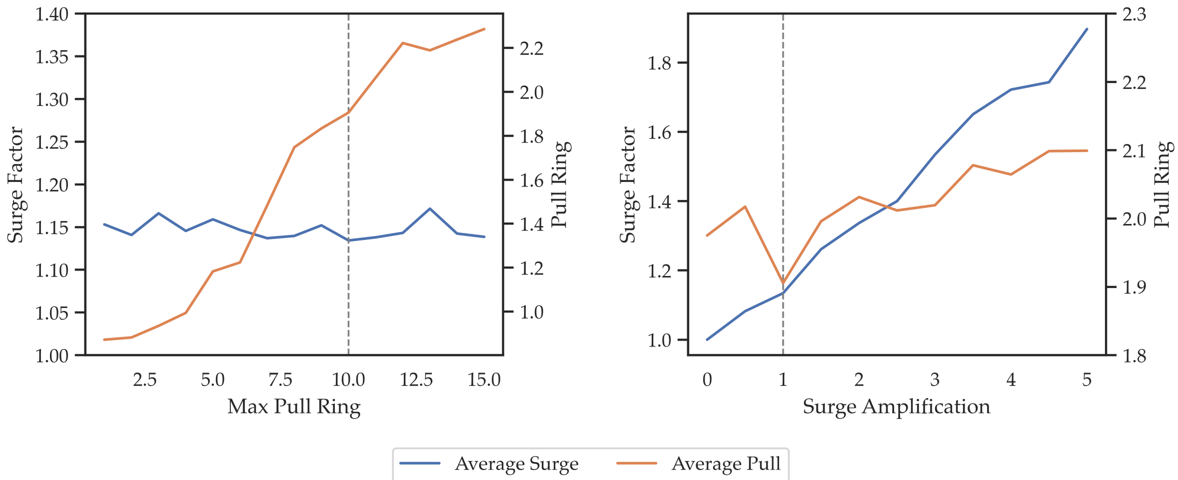

Table F13: Varying Matching and Surge Simultaneously

	Benchmark	Platform Commission	Flexible Surge
Consumer Surplus	286,105.81	266,294.52	321,905.75
Driver Profit	49,345.83	33,128.75	64,197.76
Platform Profit	5,848.00	5,588.00	10,702.00
Total Welfare	341,299.65	305,011.27	396,805.51
Total Rides	5,848	5,588	10,702
Driver Count	2,596	2,232	2,842
Average Surge	1.13	1.19	0.67
Fraction Surge	0.23	0.28	0.13
Vacant Time	6.88	7.01	4.24
Average Pull	1.91	2.03	1.55

Notes: Benchmark indicates the baseline model that was estimated. Platform commission is a counterfactual where the platform receives 25% of the fare. Flexible surge is a counterfactual where surge is allowed to go below 1.